October 28, 2002

Dynamics of magnetic flux tubes in giant stars and close binary stars

Volkmar Holzwarth, Max–Planck–Institut für Aeronomie

1. Magnetic flux tube model

2. Flux tubes in giant stars

3. Flux tubes in close binaries

4. Drag instability

The active Sun

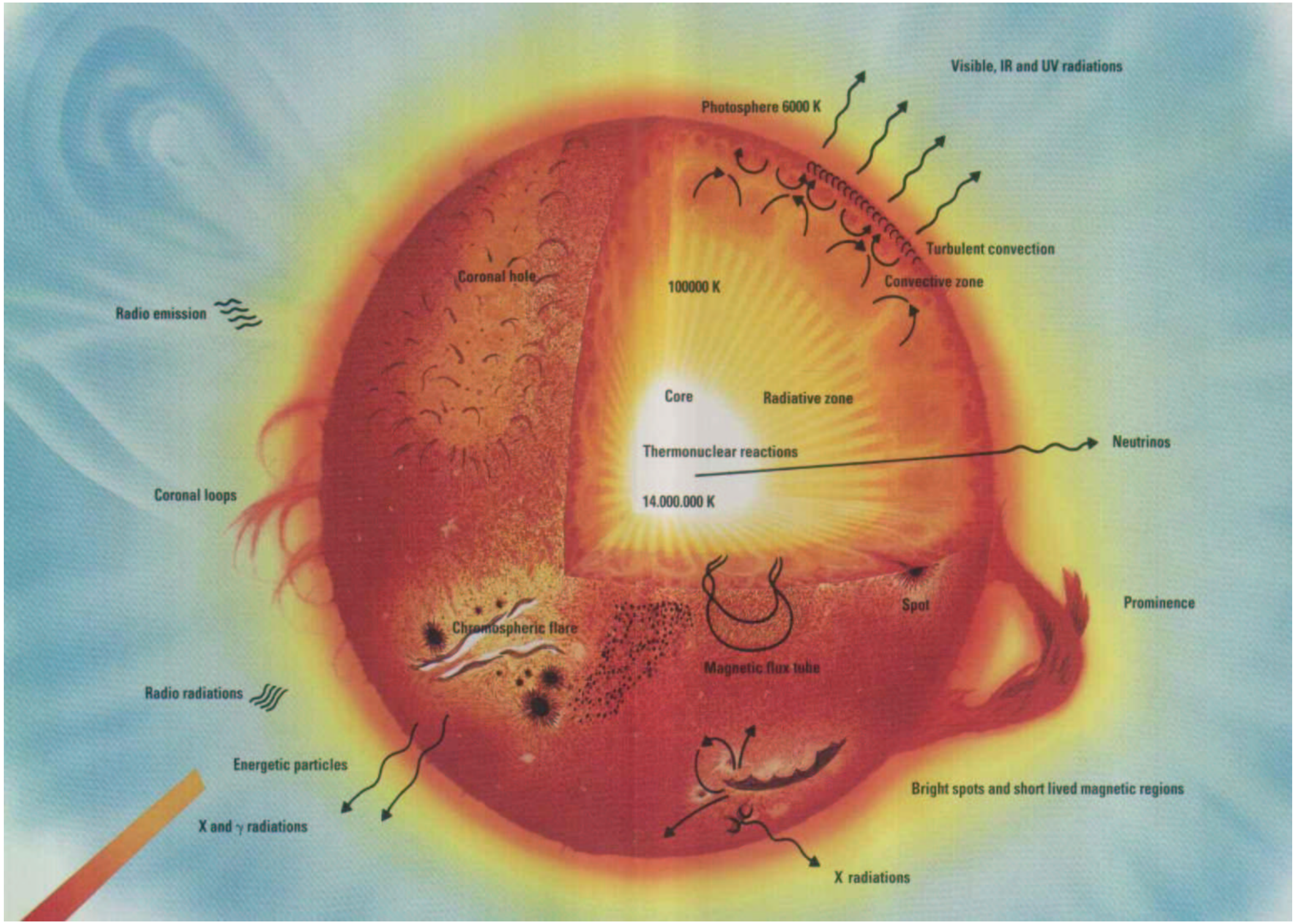

Flux tube model

- *Storage of magnetic flux:*
  toroidal flux tubes in mechanical equilibrium in the overshoot-region, parallel to the equatorial plane
- *Evolution:*
  instabilities lead to formation of **rising** flux loops

⇒ **Flux eruption** at solar surface and **magnetic activity**

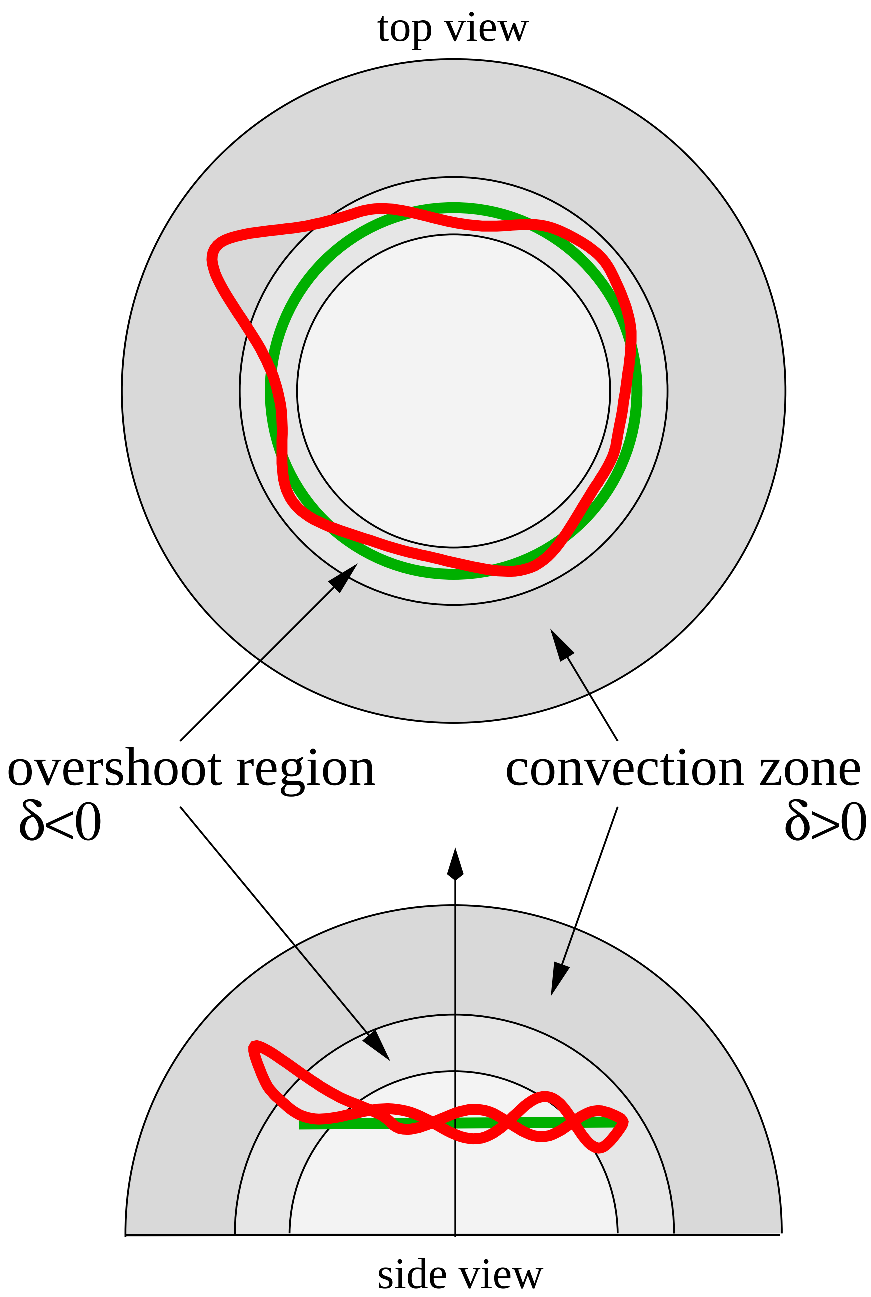

Mechanical equilibrium

- *Assumption:* Stationary flux tube with internal flow, parallel to equatorial plane

$$\begin{aligned} \rho_{\rm i} &= \rho_{\rm e} \\ R &= \text{const.} \\ \mathbf{v}_{\rm i} &> \mathbf{v}_{\rm e} \end{aligned}$$

$\Rightarrow$ **non-buoyant** flux ring, curvature force balanced by Coriolis force

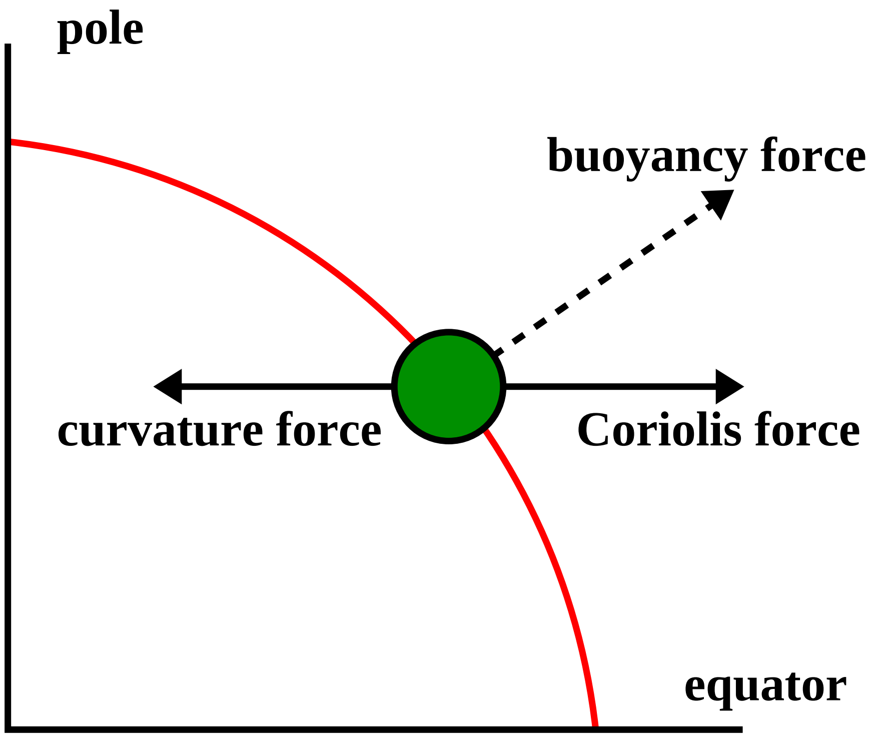

Linear stability analysis

- *Eigenvalue problem:*

  Decomposition of displacements $\xi = (\xi_{\mathrm{t}}, \xi_{\mathrm{n}}, \xi_{\mathrm{b}})^T$ in eigenmodes

$$\xi(\phi, t) = \hat{\xi} e^{i(m\phi + \omega t)}$$

  with eigenfrequency ω and azimuthal wave number m

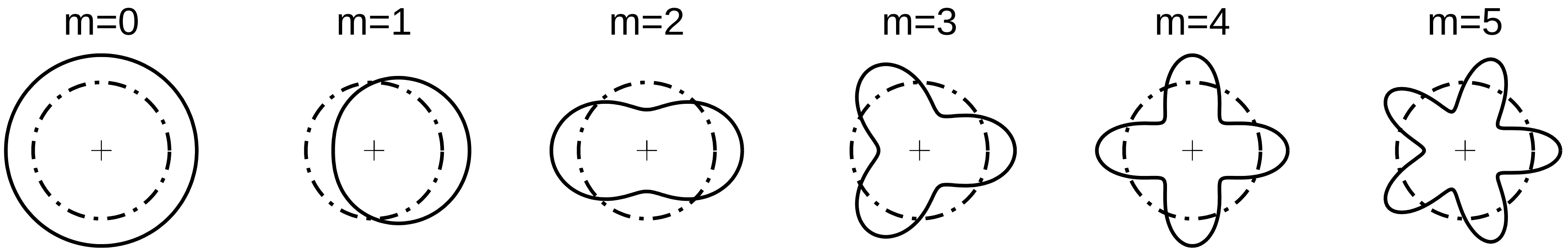

- If critical magnetic field strength B_{crit} is exceeded: $\Im(\omega) < 0$

$\Rightarrow$ **Unstable** perturbations and formation of rising flux loops

Stability diagram

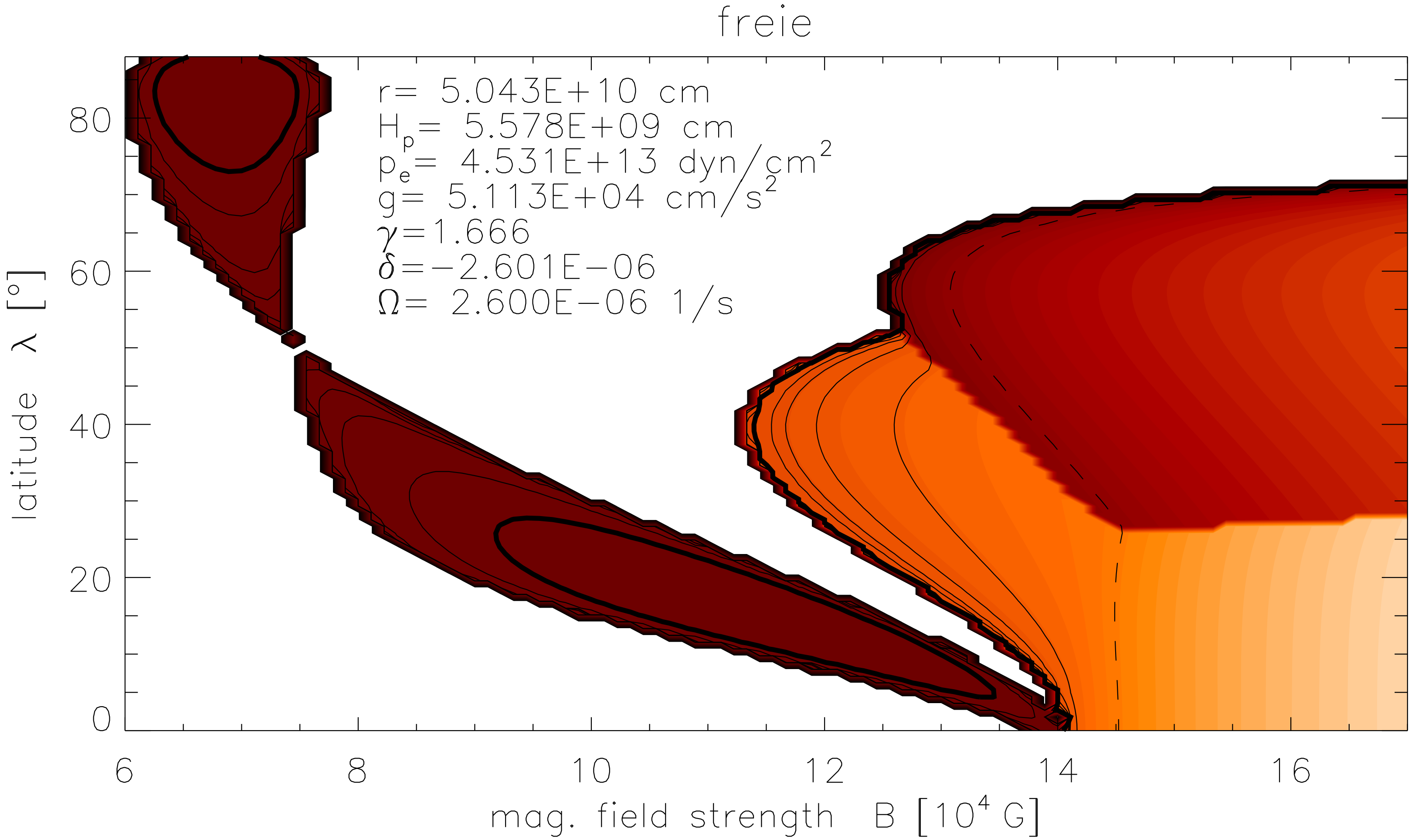

contour levels: $\tau = 10$ (dashed), $20, 30, 40, 50, 100$(thick), $150, 300, 500, 10^3, 10^4, 10^5$ d

dark shading: $m = 1$, light shading: $m = 2$

Non-linear evolution and eruption

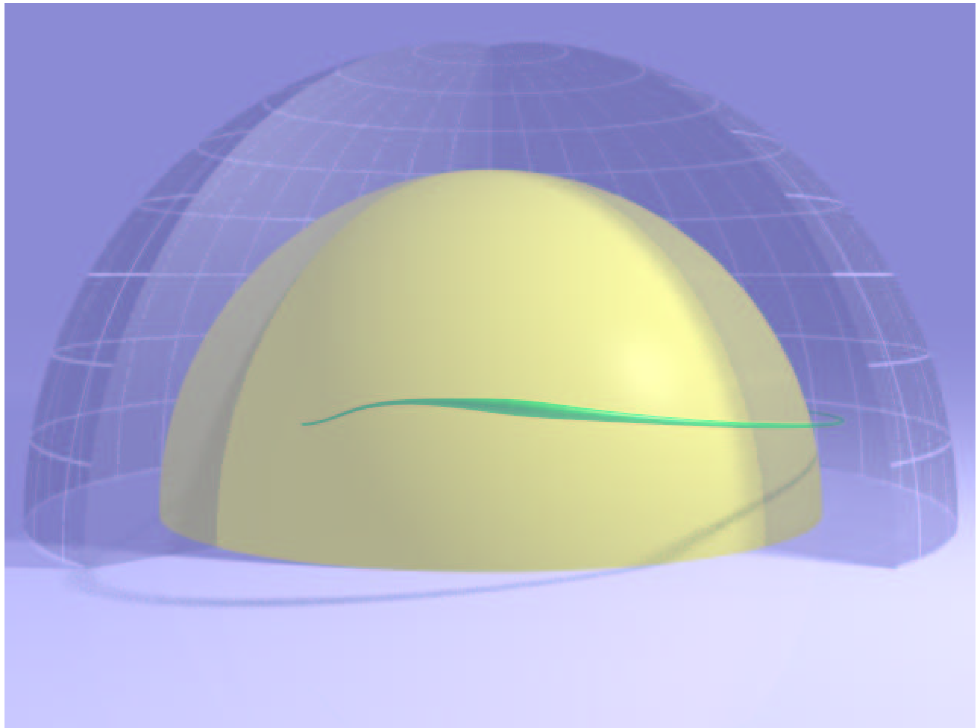

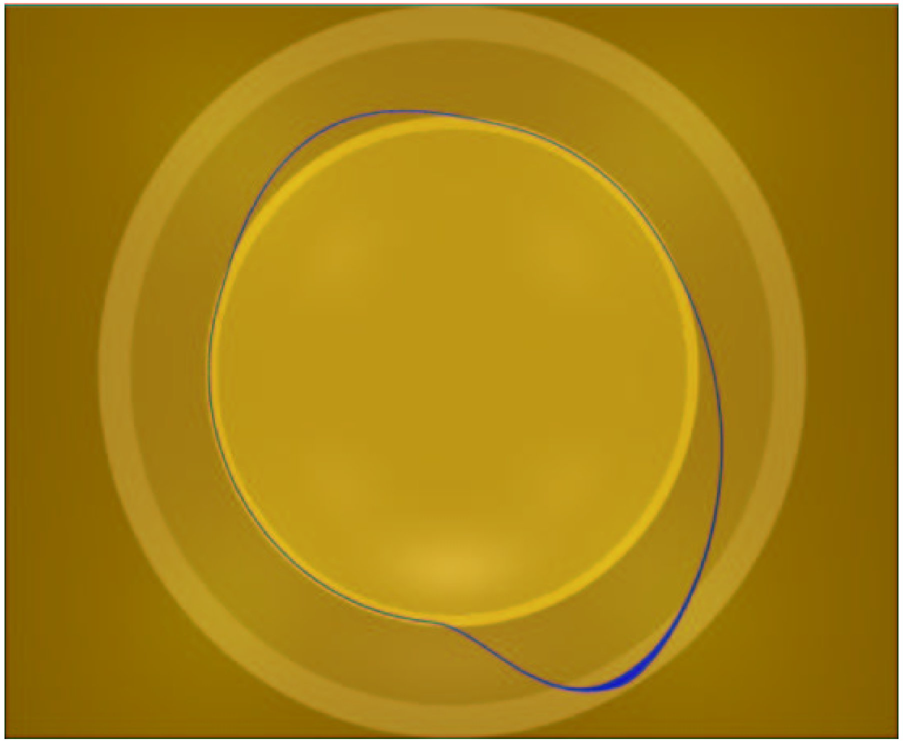

P. Caligari, Diss. 1995, Uni Freiburg

Magnetic flux tubes in binaries: WHY?

- Close binaries with cool, evolved components:

fast rotation and **deep** convection zones	$\Rightarrow$	**strong** magnetic activity (e.g., RS CVn and BY Dra systems)

- *Observations:*
  - huge starspots covering $> 20\%$ of visible hemisphere
  - spots at high and polar latitudes (*polar caps*)
  - non-uniform surface coverage: spot clusters at *preferred longitudes*, frequently in opposite quadrants

$\Rightarrow$ Investigation of **influence of tidal effects** on flux tube dynamics and surface distribution of starspots

Binary model

- *Assumptions:*
  - close (detached) system with active component $M_* = m\,\mathrm{M}_\odot$ and companion star $M_\mathrm{co} = qM_*$ on **circular** orbits
  - spin axes parallel, synchronized rotation
  - Kepler's law with $m = 1, q = 1, \mathbf{T = 1 \ldots 10}\,\mathrm{d}$
    $\Longrightarrow$ separation $a \simeq 5 \ldots 25\mathrm{R}_\odot$
  - active star: **'perturbed'** single star model
    companion star: point mass

Influence of companion star

- Tidal effects treated in **lowest-order** perturbation theory:
  - deformation of the stellar structure $\Psi_{\rm tide}/\Psi_* \propto \epsilon^3 \cos{(2\phi)}$
  - tidal forces, e.g., $g_{{\rm eff},\phi}/g_* \propto \epsilon^3 \sin{(2\phi)}$
  - $\epsilon^3 = \left(\frac{r}{a}\right)^3 \sim 10^{-2} \ldots 10^{-4}$

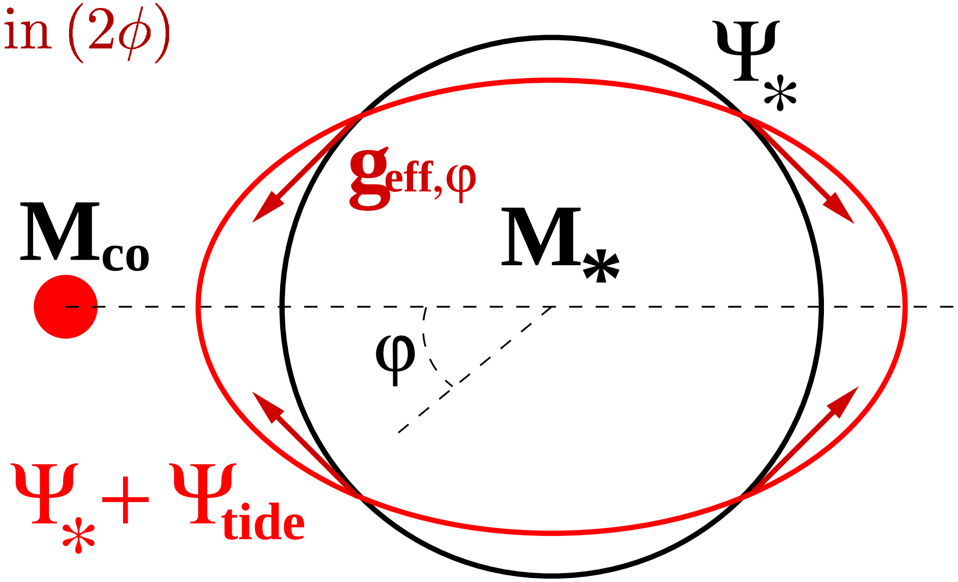

$\Rightarrow$ π**-periodic** dependence of tidal effects on longitude ϕ

Binary model

- *Assumption:* close detached system, circular orbits, synchronized rotation; stellar masses $M_* = M_{\rm co} = 1\,{\rm M}_\odot$ and orbital periods $T = 1 \ldots 5\,{\rm d}$, $\Rightarrow$ separation $a \sim 5 \ldots 15\,{\rm R}_\odot$
- Tidal effects treated in **lowest-order** perturbation theory
  - deformation of the stellar structure:
    $\Psi_{\rm tide}/\Psi_* \propto \epsilon^3 \cos(2\phi)$
  - tidal forces:
    e.g. $g_{{\rm eff},\phi}/g_* \propto \epsilon^3 \sin(2\phi)$
  - $\epsilon^3 = \left(\frac{r}{a}\right)^3 \sim 10^{-2} \ldots 10^{-4}$

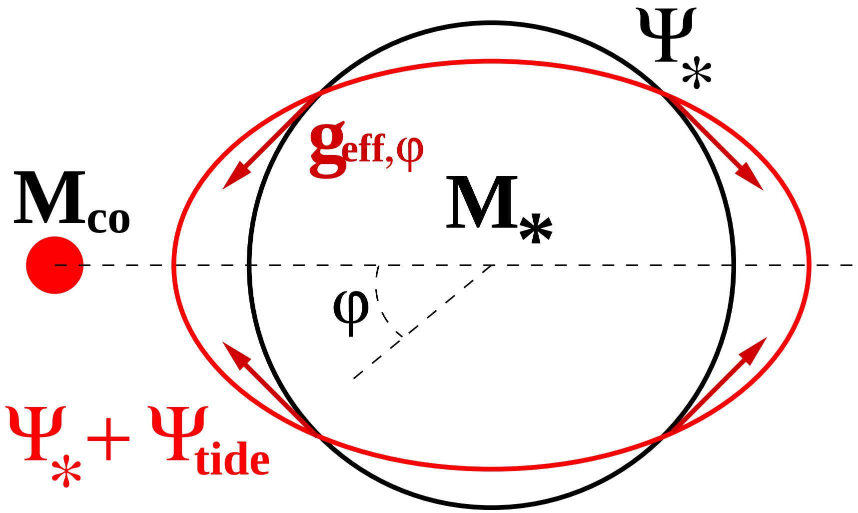

$\Rightarrow$ π**-periodic** dependence of tidal effects on longitude ϕ

Linear stability analysis

- Periodic azimuthal variation of equilibrium quantities along flux rings due to stellar deformation

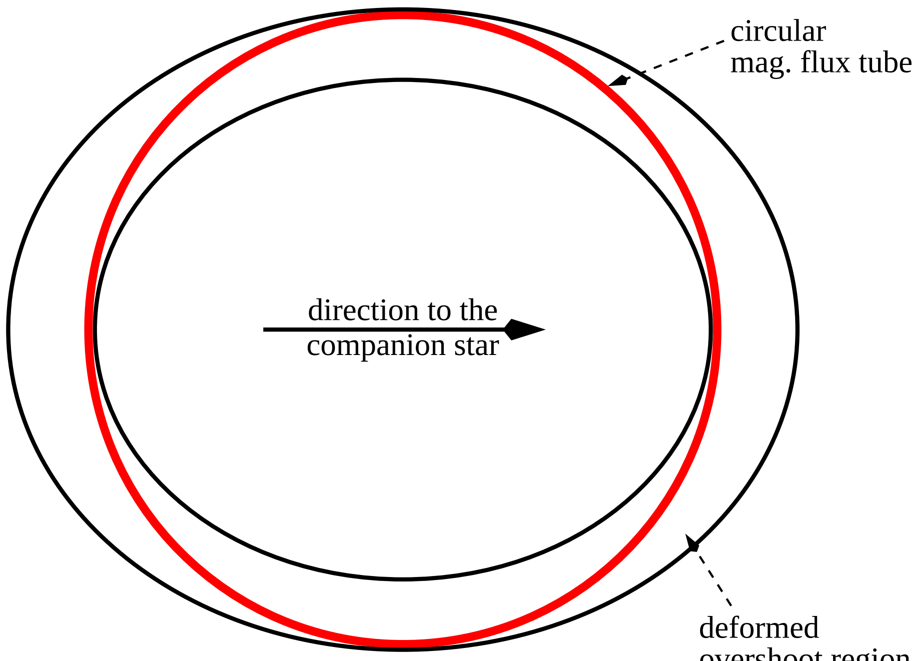

$\Rightarrow$ EV problem for displacement vector $\xi(\phi)$ and eigenfrequency ω consists of ODE's with periodic coefficients (Hill-type problem)

$\Rightarrow$ Solutions $|\xi| = |\xi(\phi)| \neq \text{const.}$, i.e., envelope varies with longitude (cf. single star: $|\xi| = \text{const.}$, i.e., constant envelope at all longitudes)

Eigenvalue problem

- Linearized equation of motion for small displacement $\xi(\phi, t)$:

$$\xi'' + \left[\mathcal{M}_\phi + i\omega\mathcal{M}_{\phi t}\right]\xi' + \left[\mathcal{M}_\xi + i\omega\mathcal{M}_t - \omega^2\mathcal{M}_{tt}\right]\xi = 0$$

with

$$\xi(\phi + 2\pi) = \xi(\phi) \quad , \qquad \xi'(\phi + 2\pi) = \xi'(\phi)$$

and π-periodic coefficient matrices

$$\mathcal{M}_{\dots}(\phi + \pi) = \mathcal{M}_{\dots}(\phi)$$

$\Rightarrow$ Ansatz for eigenmode $\xi = (\xi_{\rm t}, \xi_{\rm n}, \xi_{\rm b})^T$

$$\xi(\phi, t) = \left(\sum_{k=-\infty}^{\infty} \hat{\xi}_k e^{ik\phi}\right) e^{i(m\phi + \omega t)}$$

Coupling of wave modes

- EV problem yields 3-term recursion formula

$$\mathcal{L}_{m+k}\hat{\xi}_{k-2} + \mathcal{C}_{m+k}\hat{\xi}_{k} + \mathcal{R}_{m+k}\hat{\xi}_{k+2} = 0 \quad , \qquad \forall k$$

$\Rightarrow$ Coupling of wave modes $n = m, m \pm 2, m \pm 4, \ldots$ due to tidal effects:

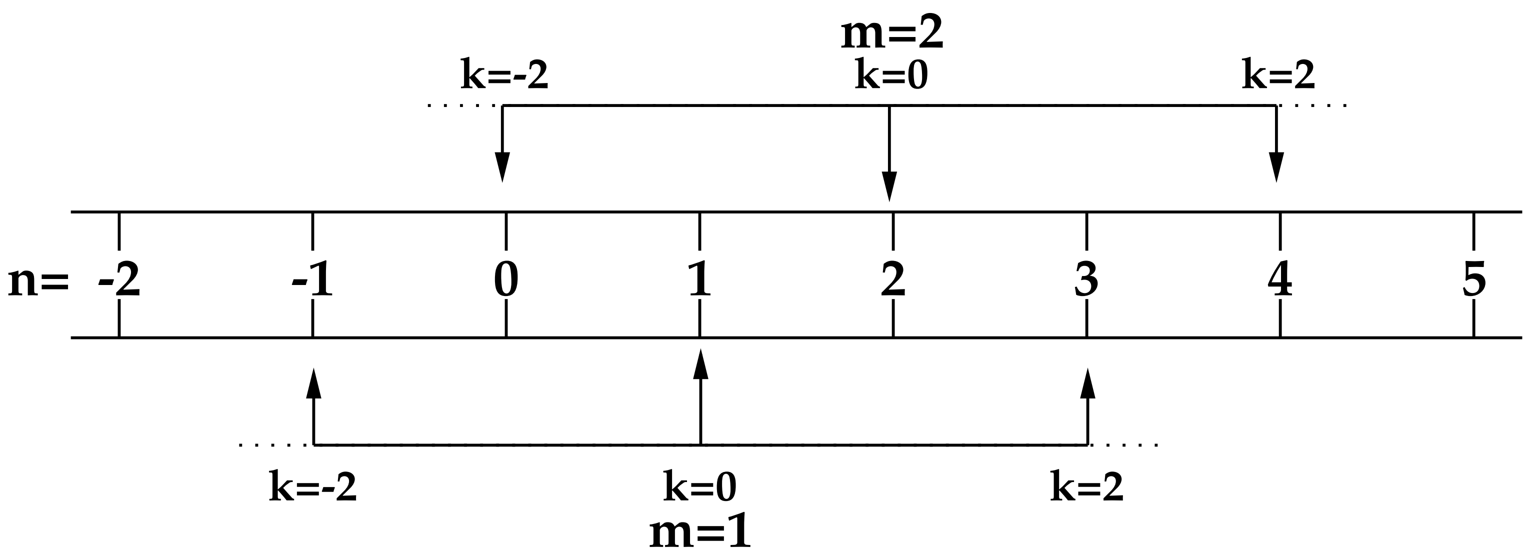

Eigenfunctions

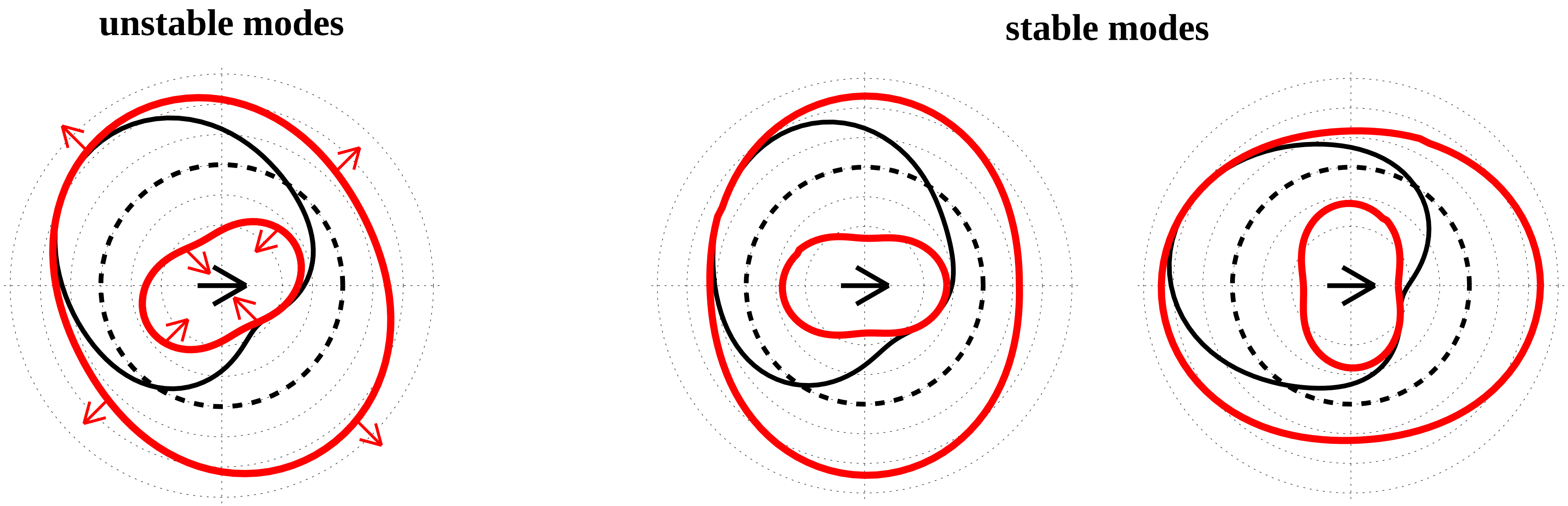

- Periodic azimuthal variation of envelope, $\Delta|\xi|/|\xi| \sim 5 \ldots 20\%$, orientation of $|\xi|_{\max}$ depends on equilibrium configuration
- *Assumption:* probability of loop formation $W_{\text{rise}} \propto |\xi|$

$\Rightarrow$ **'Preferred longitudes'** of loop formation in overshoot-region

Growth times

- *quantitative:* very small difference compared to single star results, $\mathcal{O}(\Delta\tau/\tau) \ll \epsilon^3$
- *qualitative:* ‘instability background’ with long growth times

single star

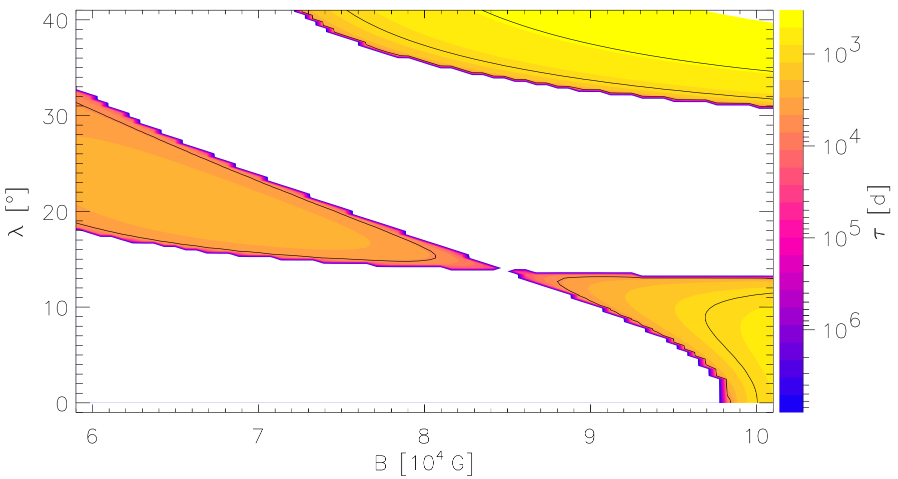

binary star

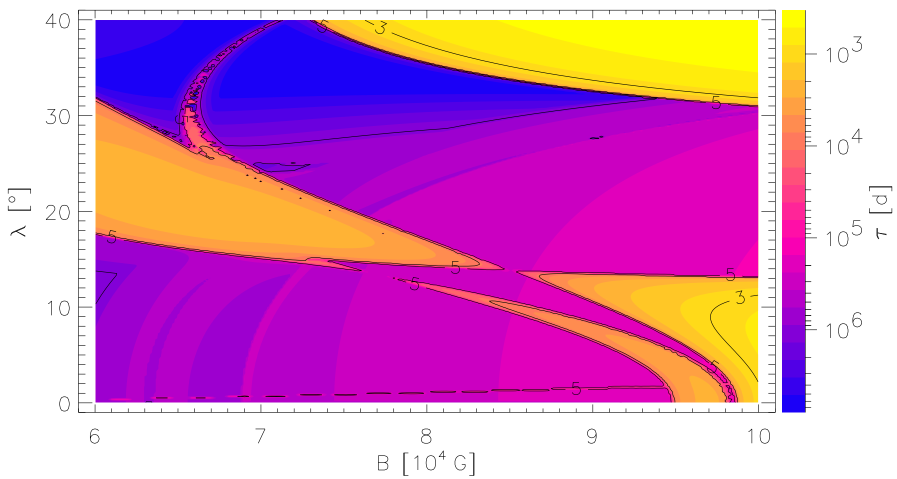

⇒ Changes in τ **insignificant** for erupting flux tubes

Resonant instabilities

- Coupling of wave modes with wave numbers n and $n+2$ due to tidal interaction
- wave modes with similar frequencies, $\Re(\omega_n) \simeq \Re(\omega_{n+2})$

$\Rightarrow$ Resonant instabilities, with long growth times and large $\Delta|\xi|/|\xi|$

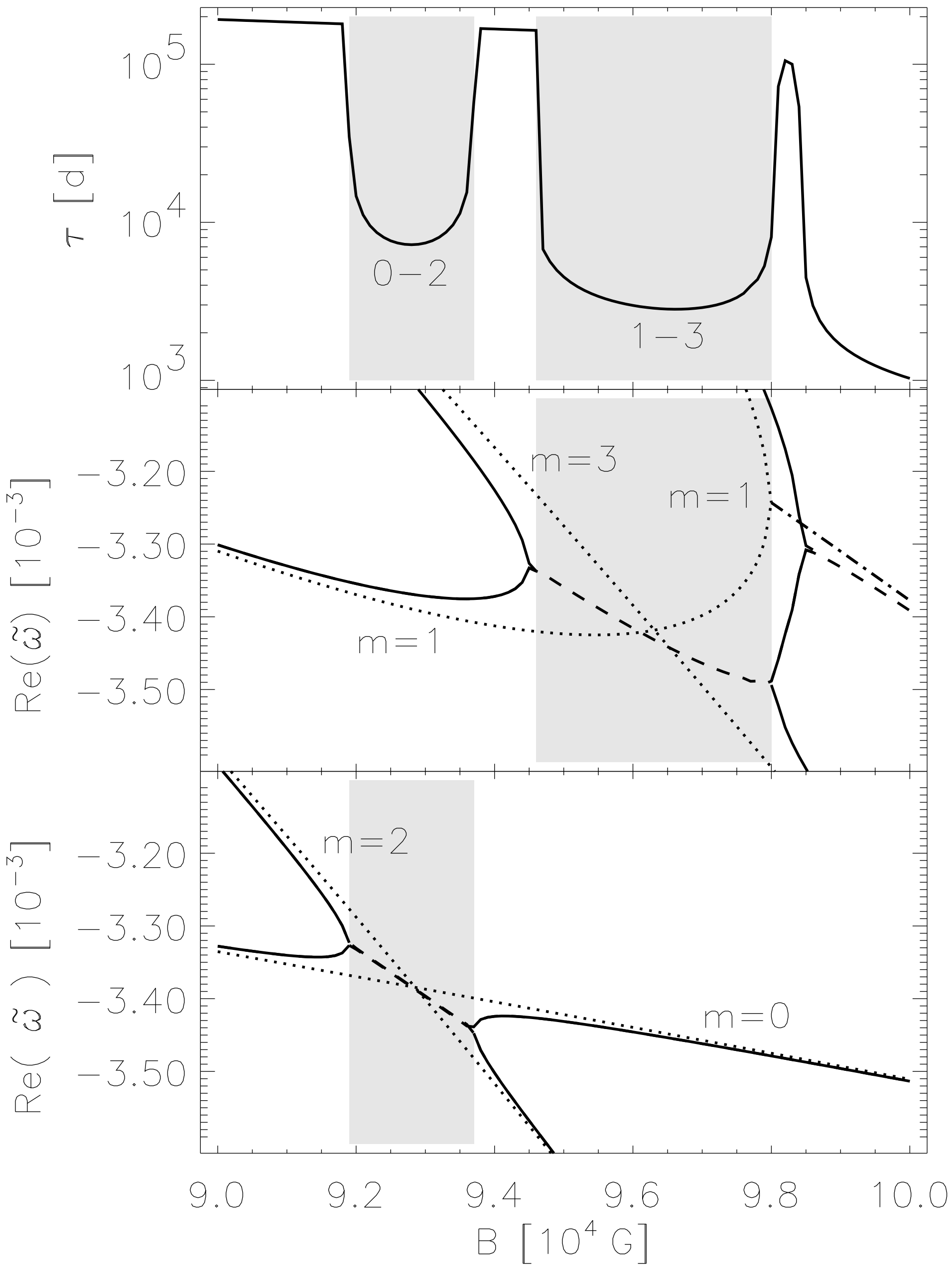

Simulations

- Sampling of longitudinal dependence of flux tube dynamics:

perturbations of the initial flux ring at $(\lambda_{\rm s}, \phi_{\rm s})$ at the ***bottom*** of the convection zone…

…lead to the eruption of a flux loop at $(\lambda_{\rm a}, \phi_{\rm a})$ at the ***top*** of the convection zone

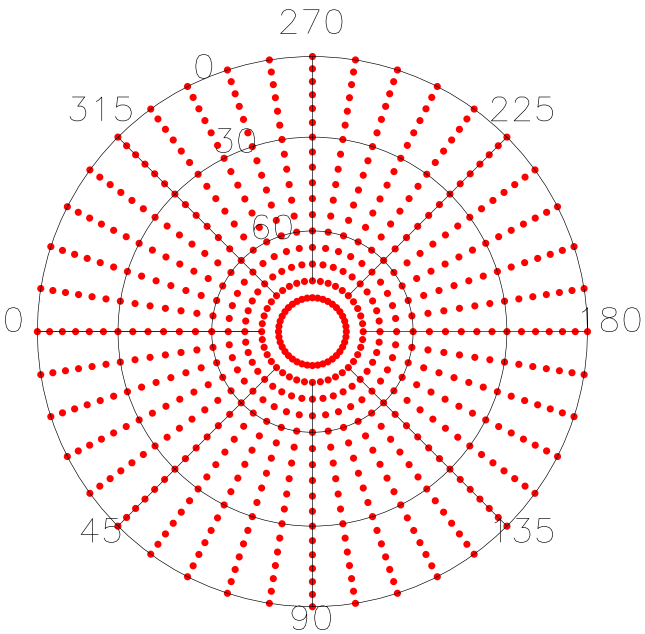

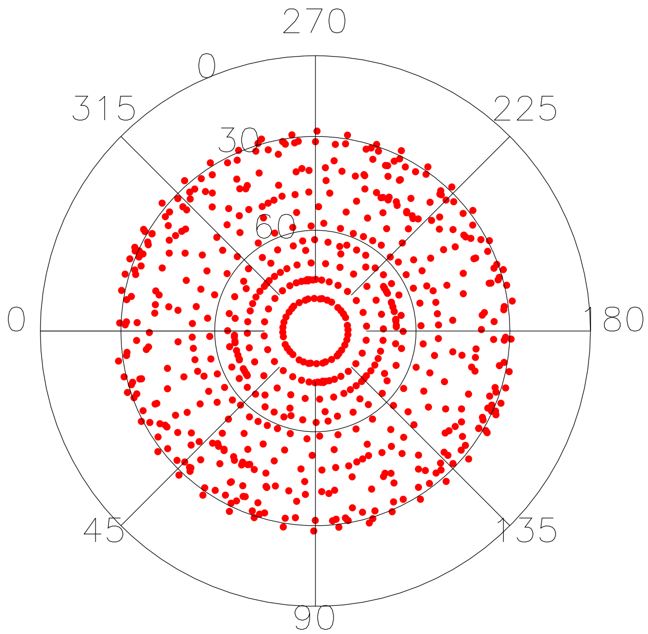

- modes of non-linear evolution:

single-loop tubes $(m = 1)$ & double-loop tubes $(m = 2)$

Localized perturbation

- in-phase superposition of wave modes with $m = 1 \ldots 5$

$\Rightarrow$ largest displacement, $\xi_{\rm max}$, at longitude $\phi_{\rm s}$

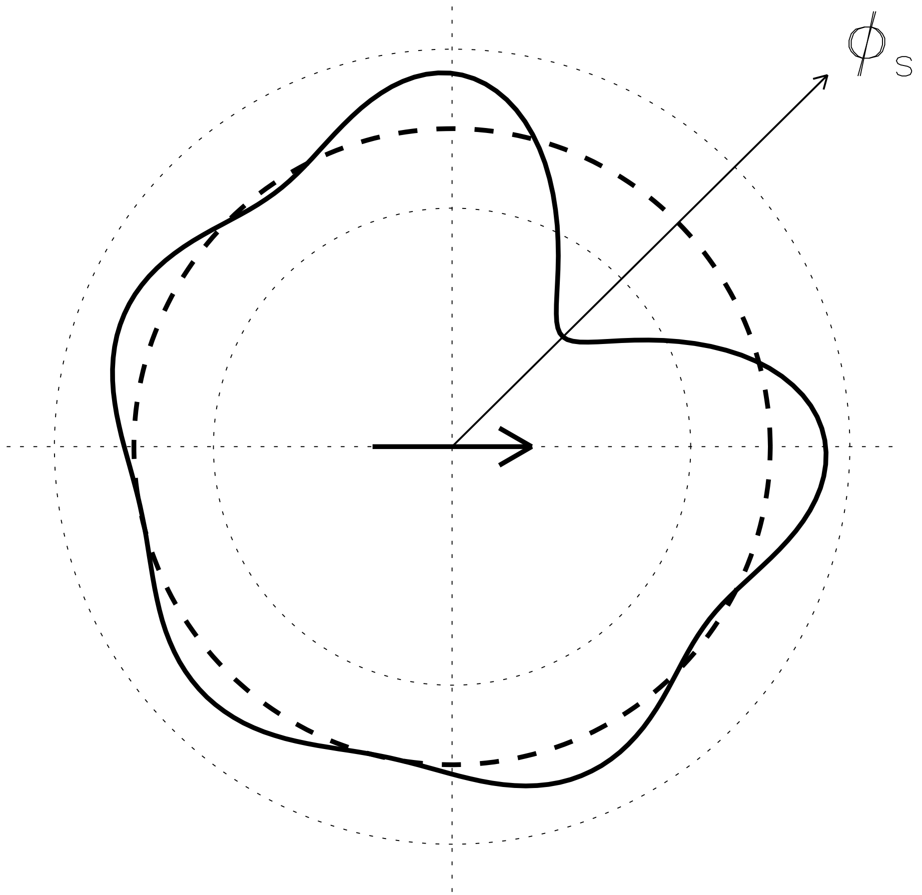

Time between perturbation and eruption (in years)

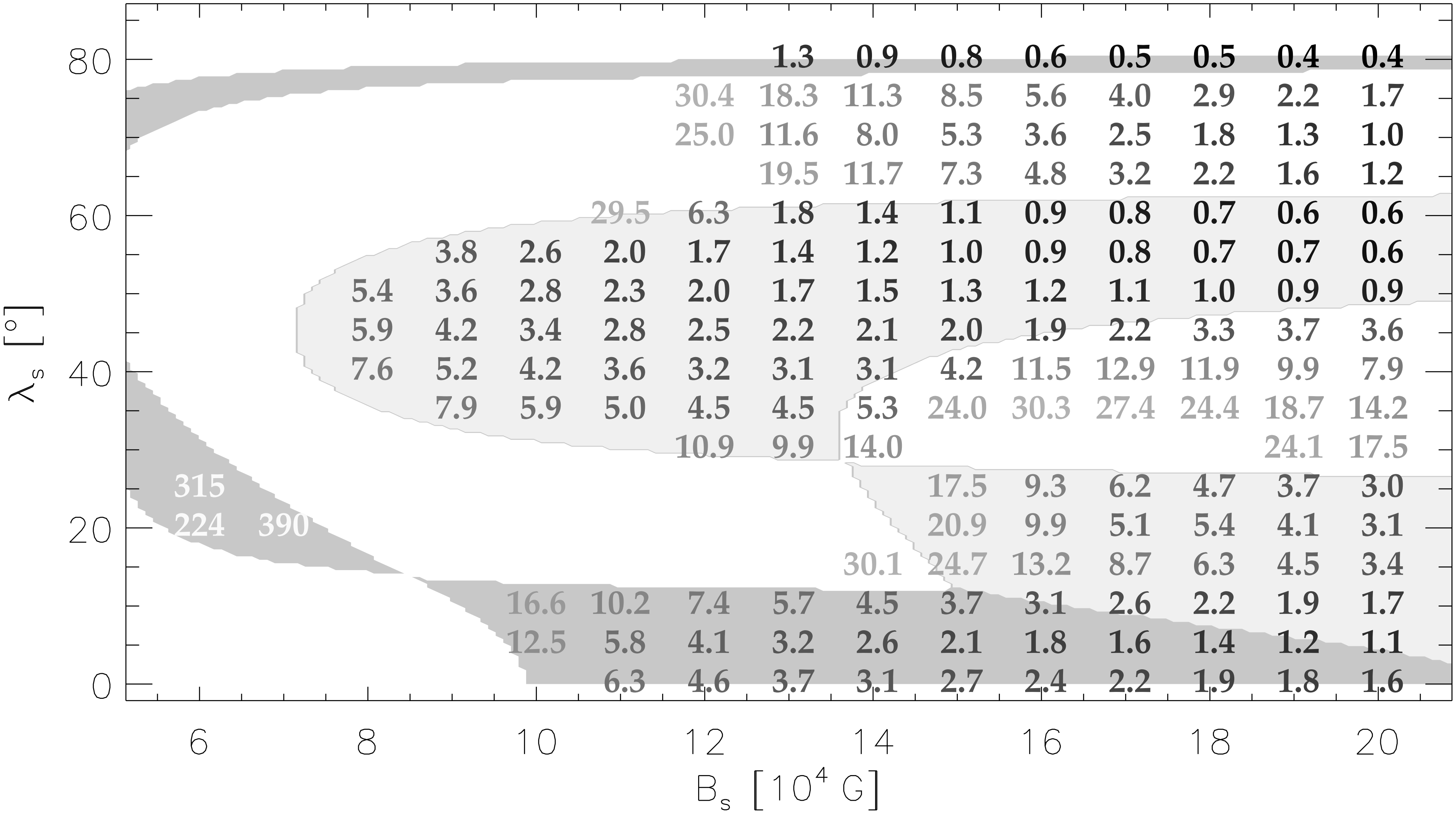

Latitudinal distribution

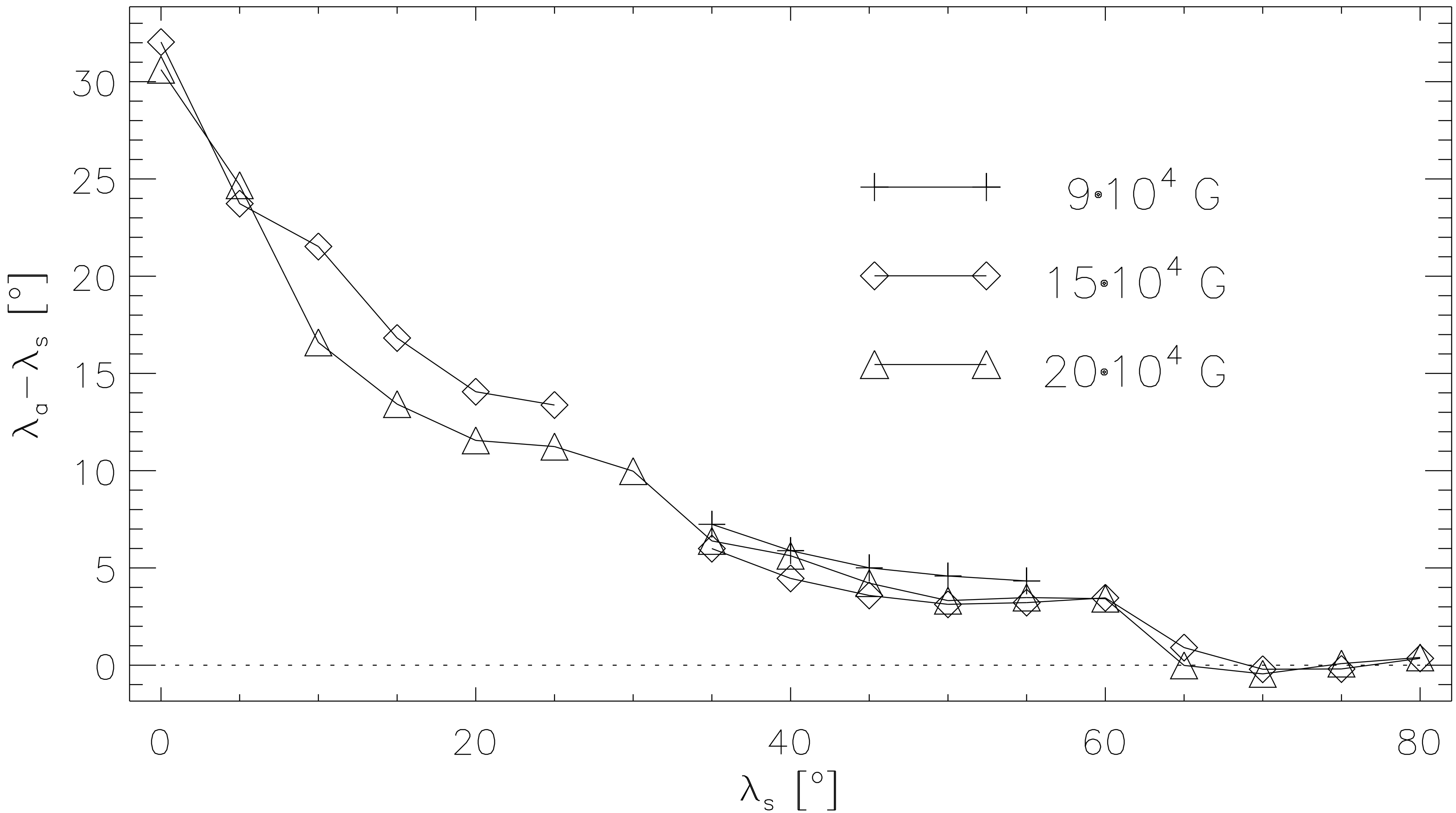

Longitudinal distribution

- in the *overshoot-region*: initial perturbation localized around longitude ϕ_s
- at the *surface*: eruption at longitude ϕ_a

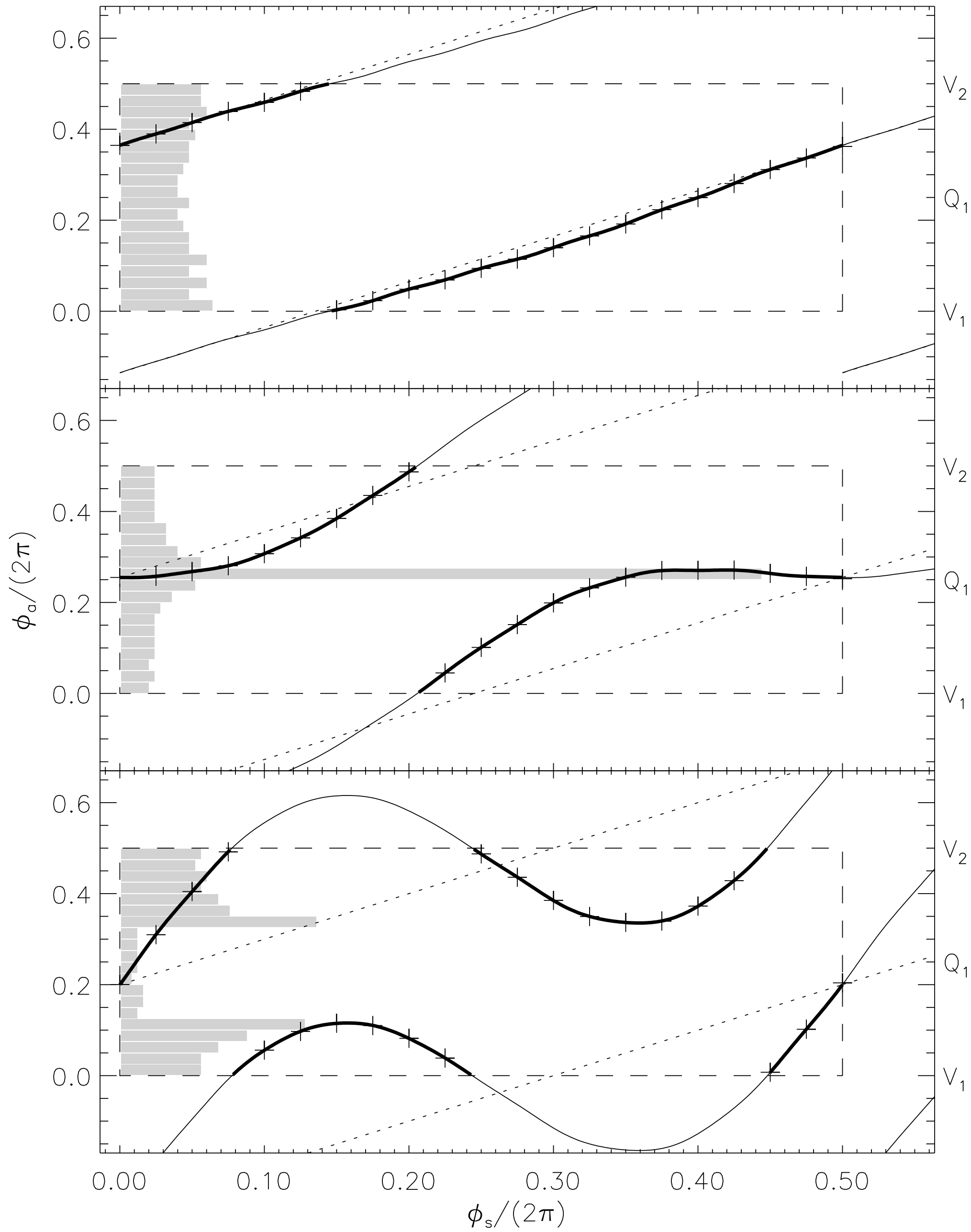

Longitudinal spot clusters

Results for $T = 2\,\mathrm{d}$

- **single-loop** tubes: insignificant asymmetries in longitudinal spot distribution
- **double-loop** tubes: considerable **non-uniform** longitudinal spot distributions
- orientations depend on initial field strength and latitude

$\Rightarrow$ **'Preferred longitudes'**

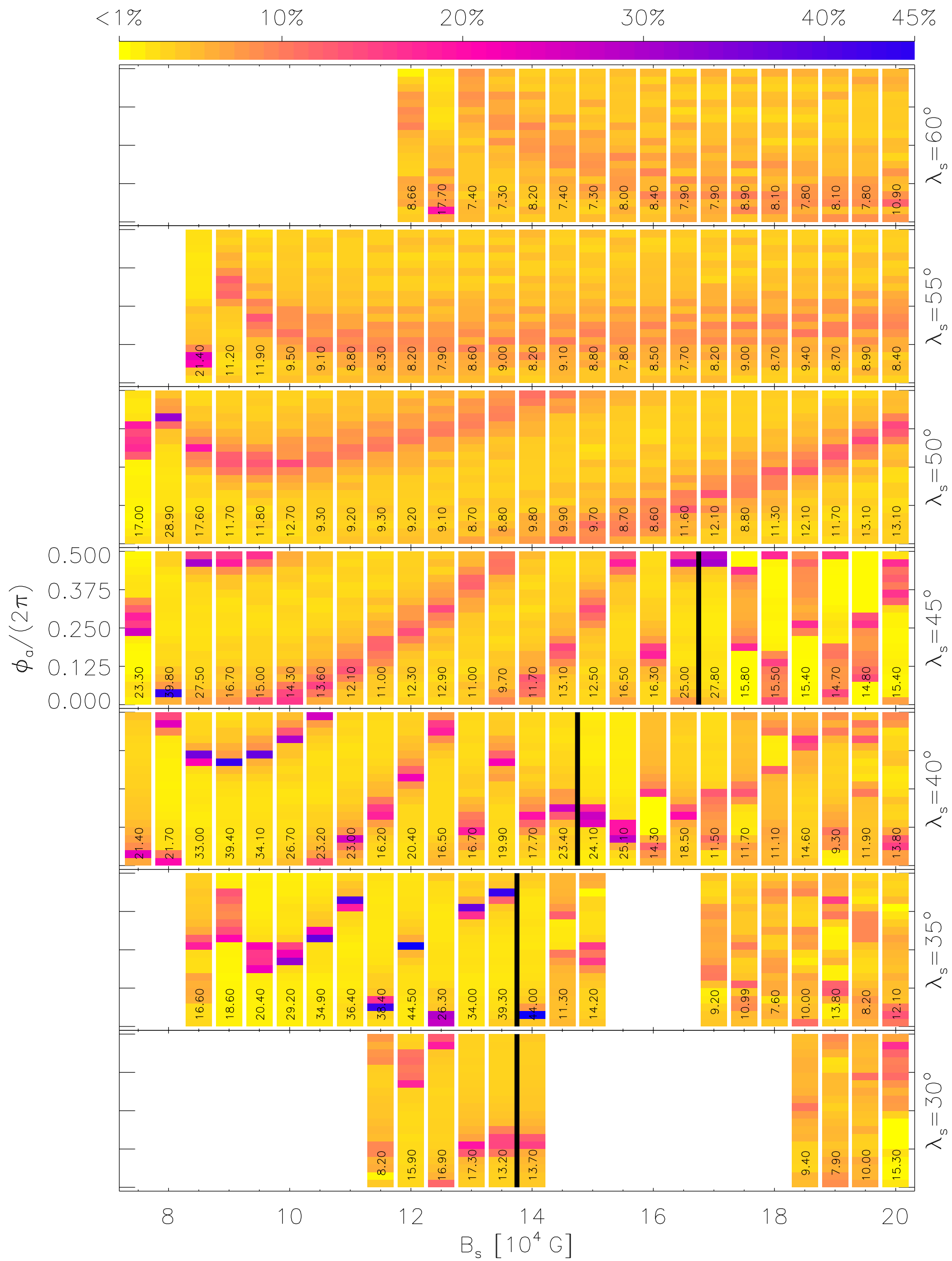

Surface distributions

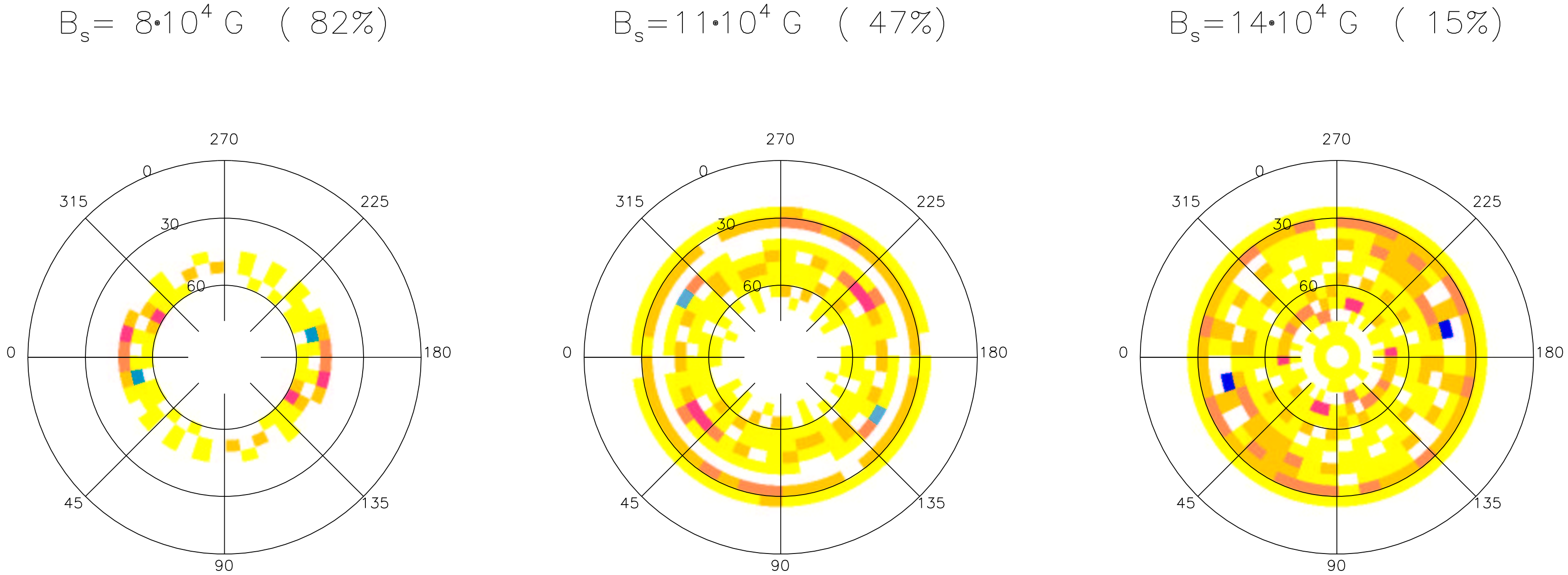

- no eruptions at **low** latitudes (below $\lambda \lesssim 25\,^{\mathrm{o}}$)
- π-periodicity of tidal effects causes spot clusters on **opposite** sides of the hemisphere

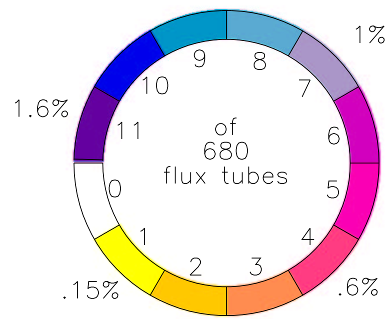

Dependence on system period T

- Strong decrease of spot clustering and tidal effects for larger system periods / binary separations

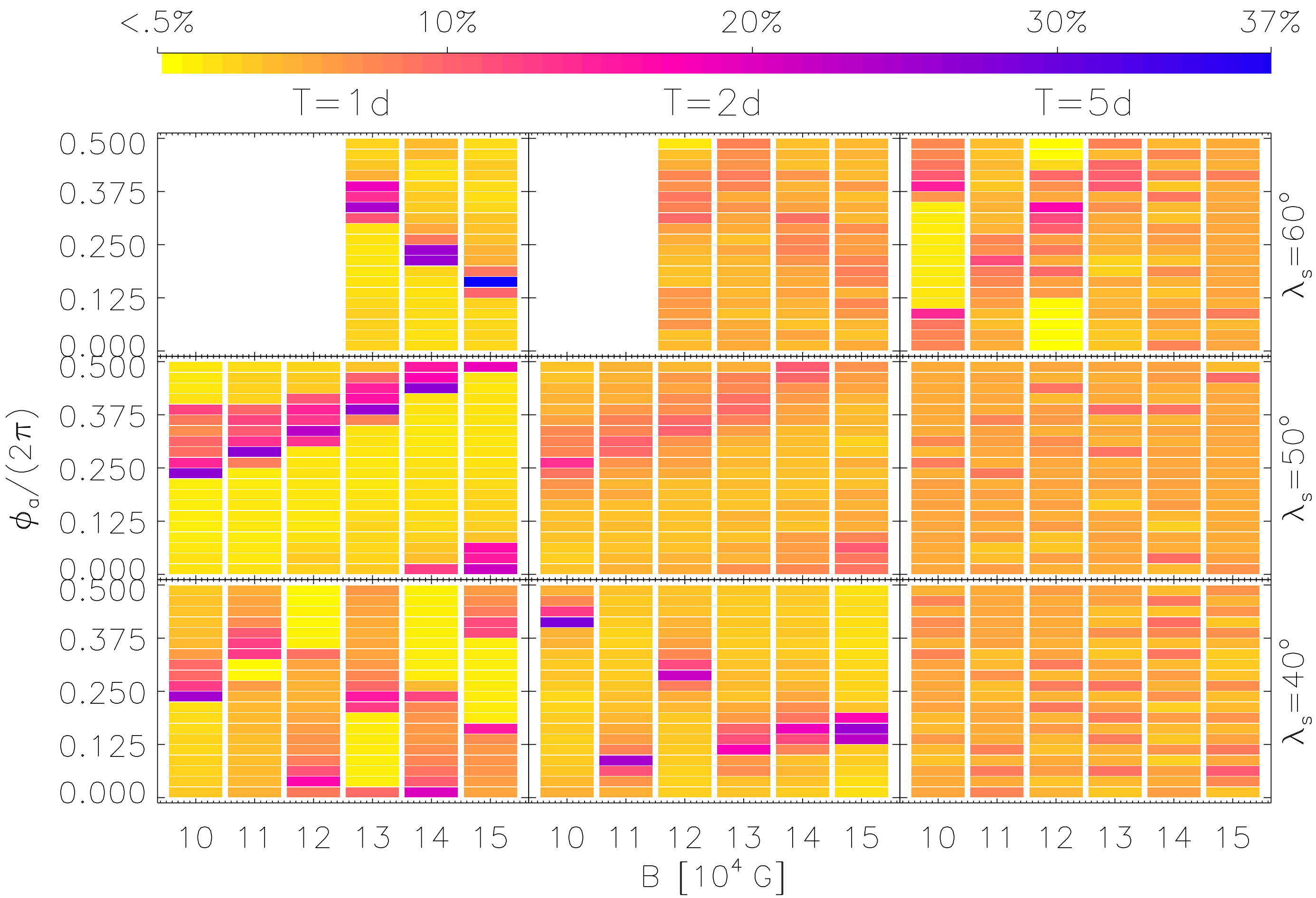

Reasons

- **Resonance effect:**
  congruency between π-periodicity of tidal effects and structure of *double-loop* flux tubes
- **Cumulative effect:**
  non-axial symmetric influence of companion star adds up during long rise (several months) until eruption

Summary

- Observations: indications for preferred longitudes in spot distribution on close binary components
- Hypothesis: preferred longitudes due to proximity effects of companion star
- Linear analysis & simulations: *preferred longitudes* exist in overshoot region and at stellar surface
- Result: small tidal effects cause considerable non-uniformities in spot distributions

$$\epsilon^3 = \left(\frac{r}{a}\right)^3 < 10^{-2} \quad \longrightarrow \quad \text{spot clusters, } \sim 180^{\circ} \text{ apart}$$

Magnetic flux tubes in giants: WHY?

Observations of giants in the HR domain K0–K3 III–IV indicate

- a significant drop of coronal X-ray emission
- the onset/increase of strong stellar winds

⇒ **‘Coronal Dividing Line’ (CDL)**

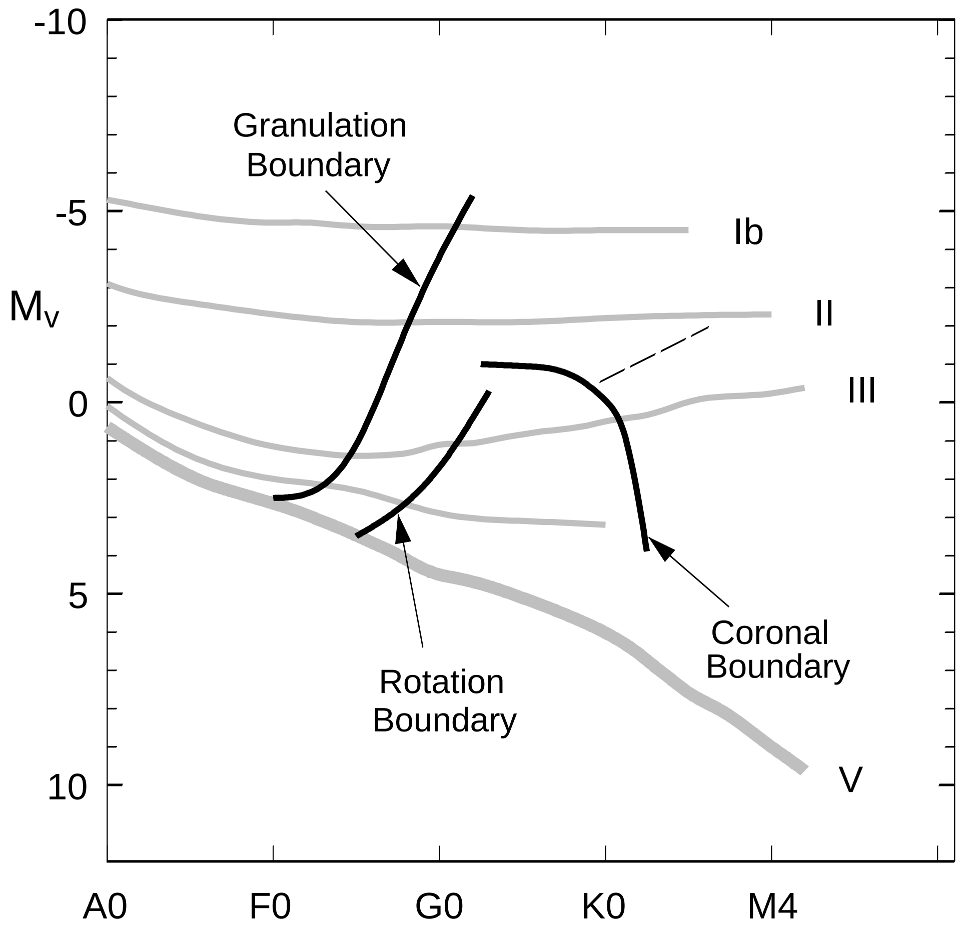

Interpretation of the CDL

Change of the **magnetic field topology** in the stellar atmosphere

closed coronal loops ↔ ‘open’ field lines

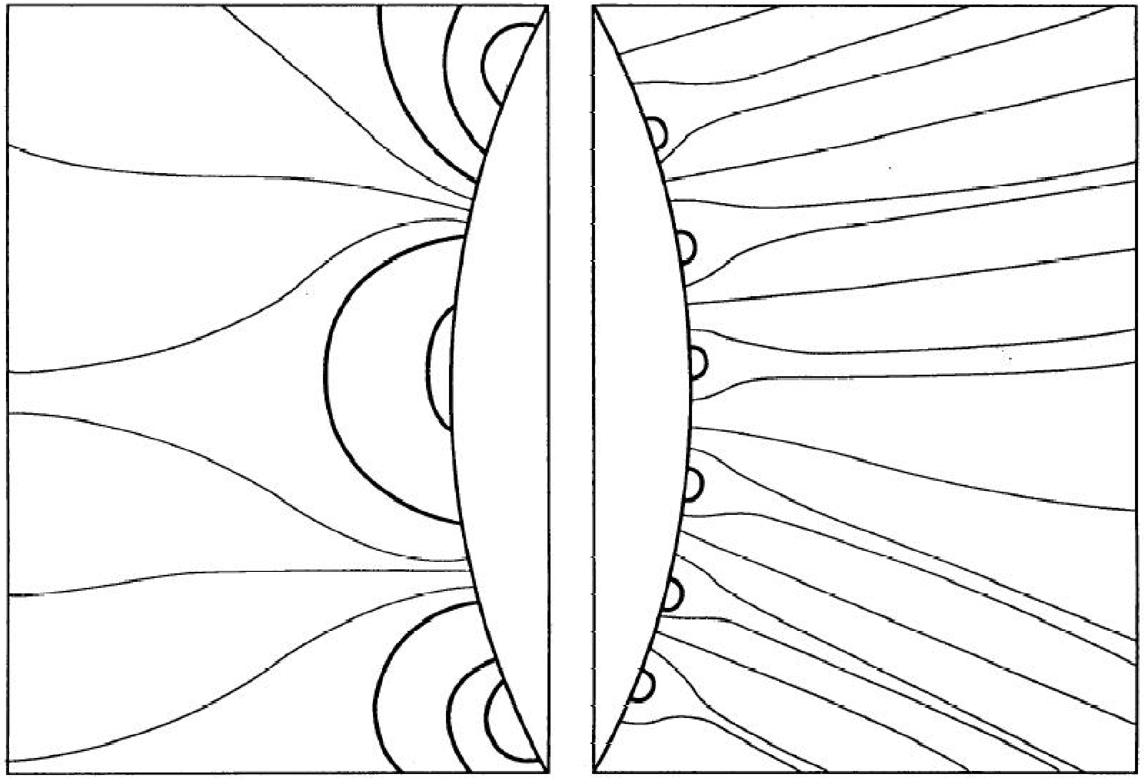

Simulations

- post-main-sequence evolution of stars with $M_* = 1 \dots 3\,\mathrm{M}_\odot$

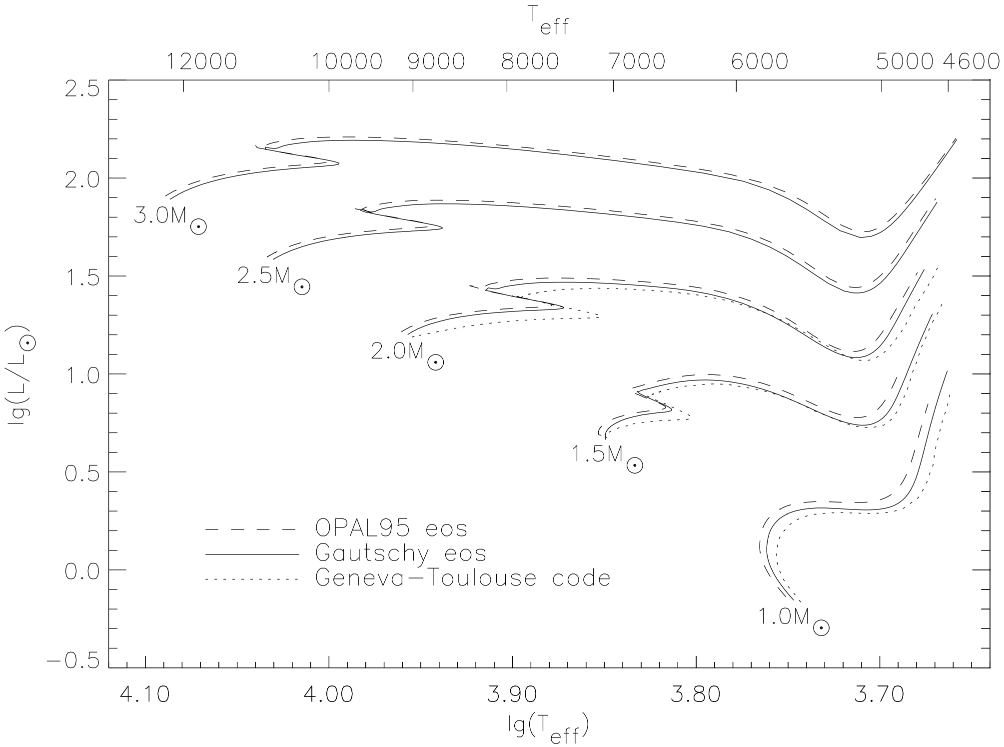

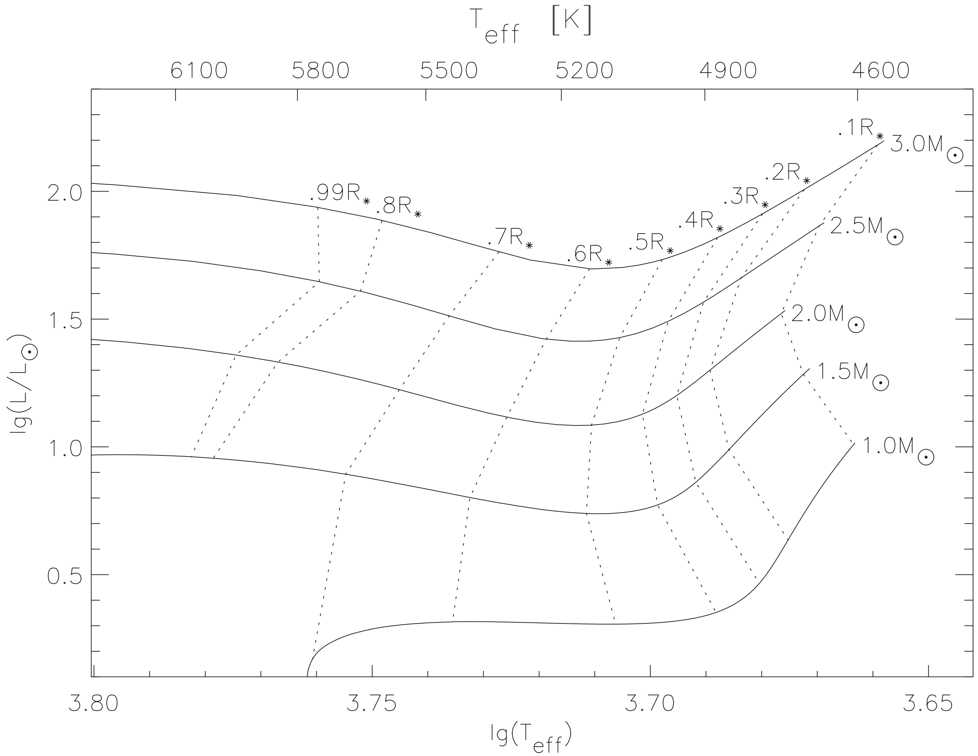

- stellar models with $0.35 \gtrsim r_{\mathrm{core}}/R_* \gtrsim 0.15$

$\Rightarrow$ flux tube model extended to post-MS stars

Erupting flux tubes

$M_* = 1\,\mathrm{M}_\odot$

$T_{\mathrm{eff}} = 4759\,\mathrm{K}$

$r_{\mathrm{core}} = 0.21\,\mathrm{R}_*$

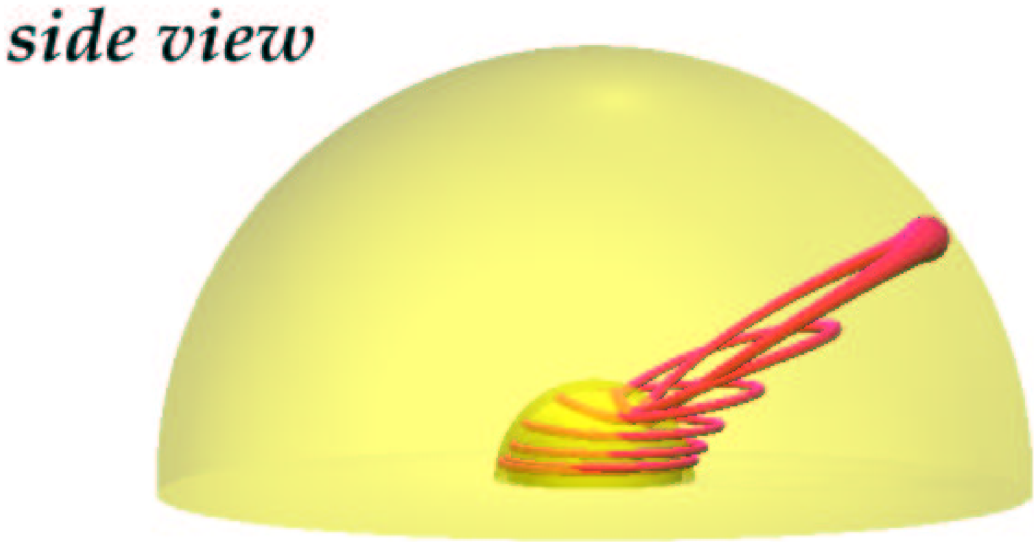

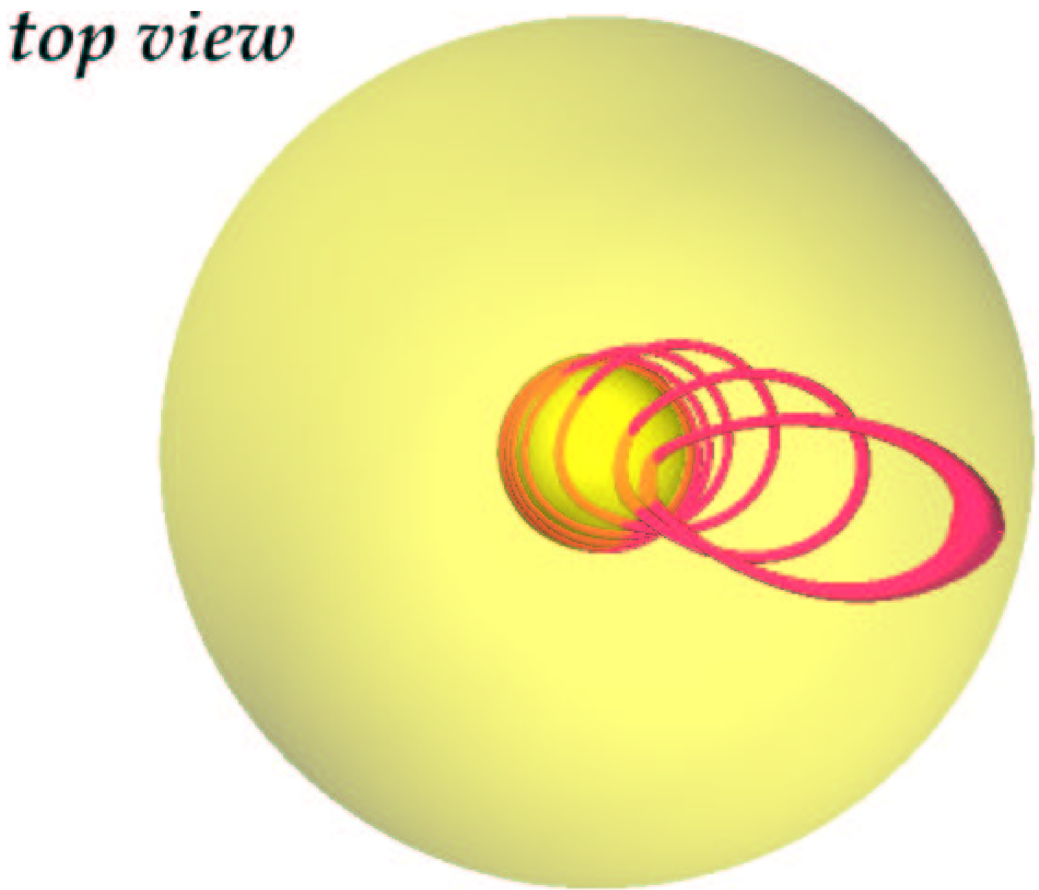

Trapped flux tubes

$M_* = 1\,\mathrm{M}_\odot$

$T_{\mathrm{eff}} = 4735\,\mathrm{K}$

$r_{\mathrm{core}} = 0.18\,\mathrm{R}_*$

top view

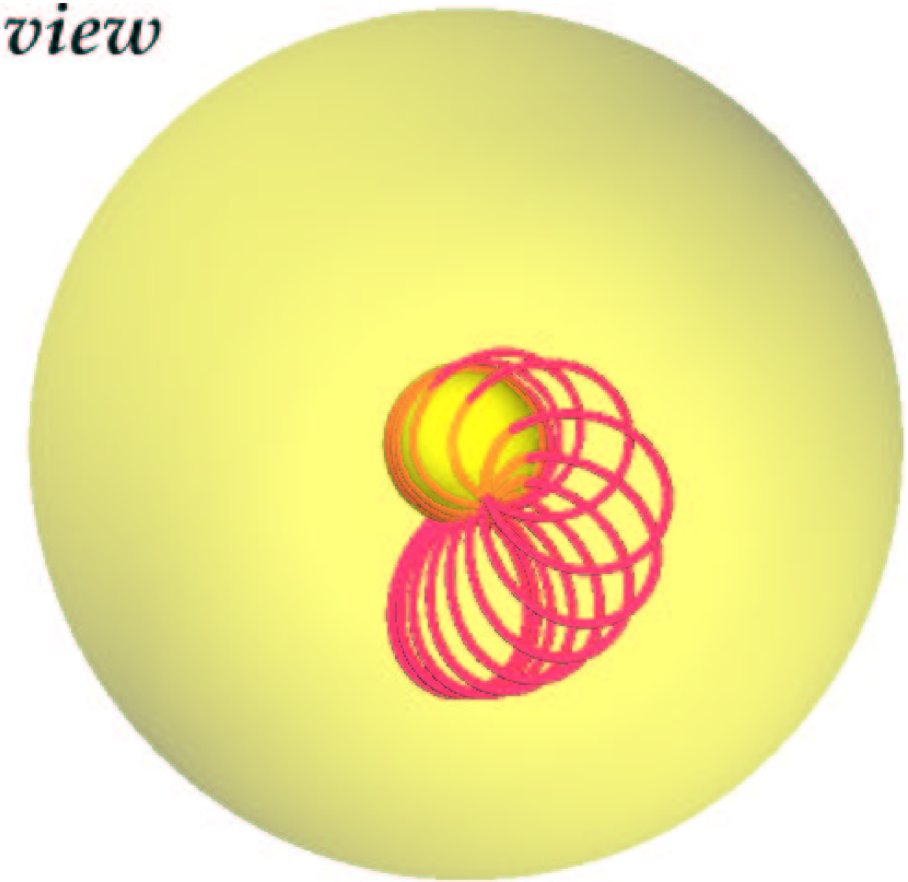

side view

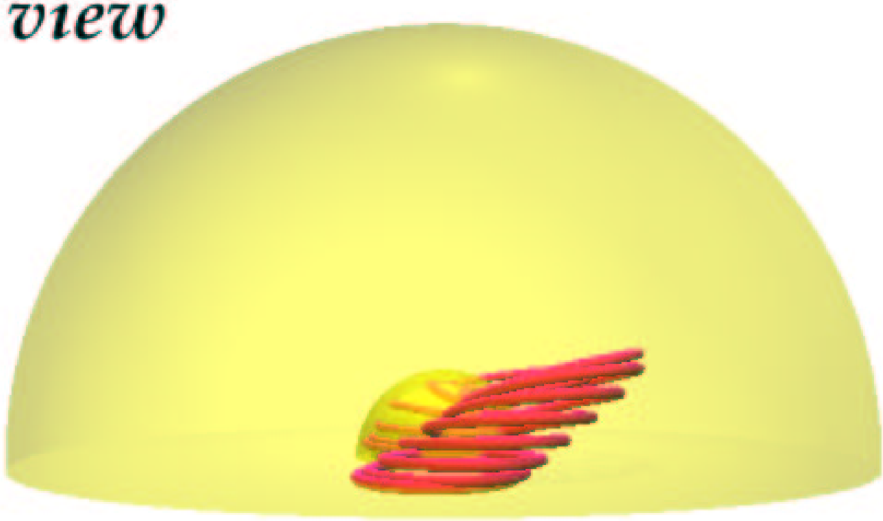

Erupting vs. buried flux tube evolution

erupting flux tube

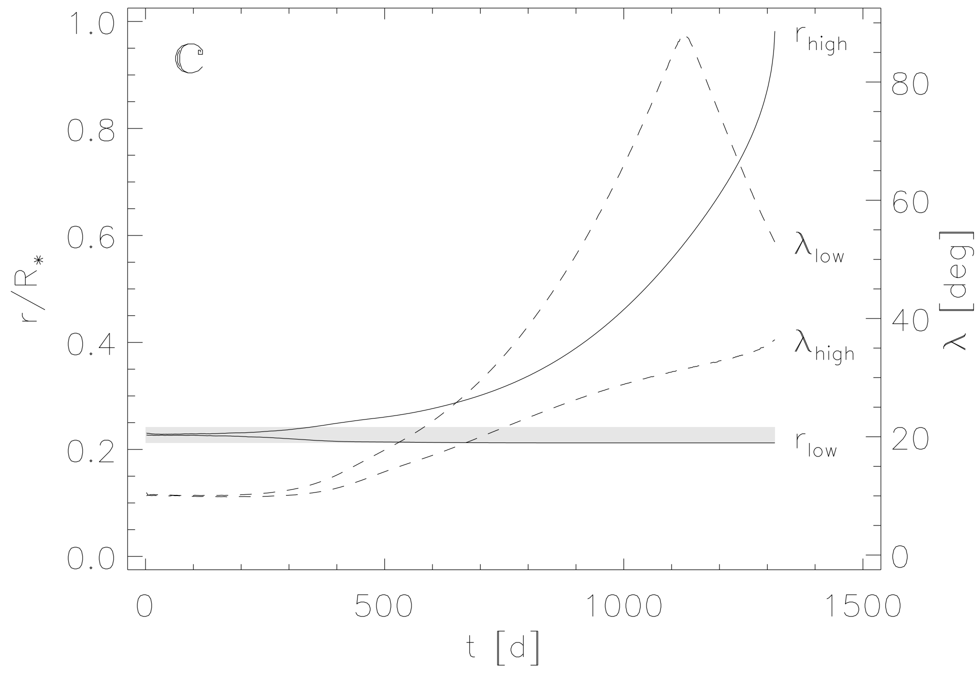

buried flux tube

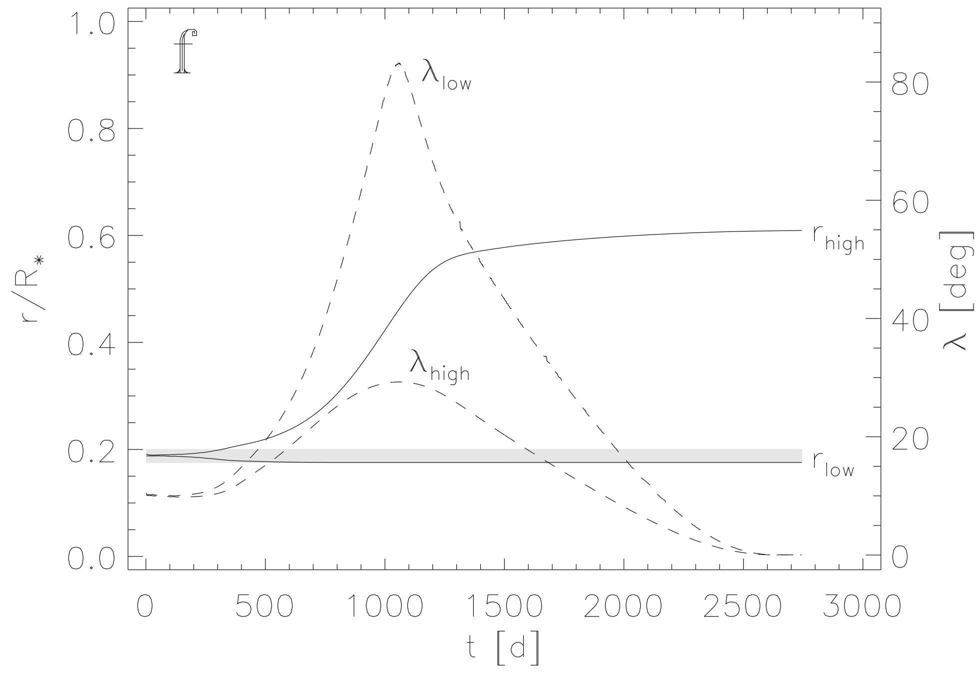

Trapping mechanism

- Forces breakdown at the crest of the rising loop:
  smaller $\mathcal{R} = R_{\rm eq}/R_{*} \Longrightarrow$ larger $\mathbf{f}_{\rm curv}$ and smaller $\mathbf{f}_{\rm buoy}$ at $r_{\rm high}$

- Force ratio at $r_{\rm high}$:

$$\frac{|\mathbf{f}_{\rm out}|}{|\mathbf{f}_{\rm in}|} = \frac{|\mathbf{f}_{\rm buoy} + \mathbf{f}_{\rm inertia}|}{|\mathbf{f}_{\rm curv} + \mathbf{f}_{\rm drag}|} < 1$$

$\Rightarrow$ rise decelerated

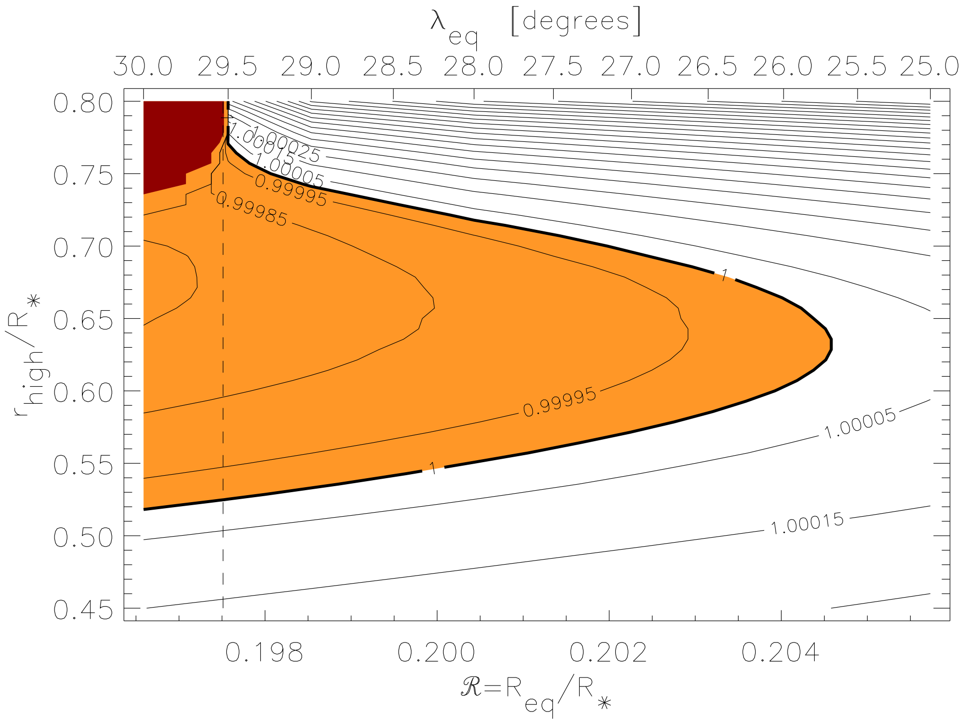

$\Rightarrow$ **Trapping** of magnetic flux tubes for $\mathcal{R} < \mathcal{R}_{\rm crit}$

Polytropic layer model

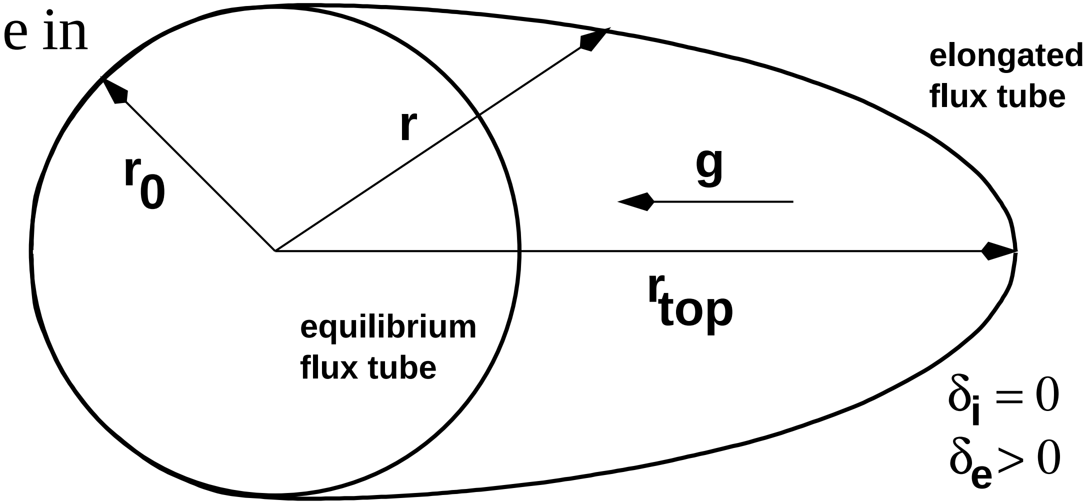

- elongated **hydrostatic** flux tube in pressure equilibrium

$$p_e = p_i + \frac{B^2}{8\pi}$$

- polytropic stratification:

$$p(r) = p_0 \eta(r)^{1/\nabla^*} \quad \text{and} \quad \rho(r) = \rho_0 \eta(r)^{1/\nabla^* - 1}$$

with $\quad g(r) \sim r^{-\sigma}, \nabla^* = \frac{\gamma^* - 1}{\gamma^*} \quad$ and $\quad \eta(r) = 1 - \frac{1}{\sigma - 1} \nabla^* \frac{r_0}{H_{p0}} \left(1 - \left(\frac{r_0}{r}\right)^{\sigma - 1}\right)$

- inside: $\nabla^* = \nabla_{ad}$ (adiab.), outside: $\nabla^* = \nabla_{ad} + \delta_e$ (superadiab.)
  $\rho_{i,0}$ is adjusted to assure conservation of mass inside the tube

Polytropic layer model vs. simulation

$|\mathbf{f}_{\rm out}/\mathbf{f}_{\rm in}|$ at uppermost tube element

polytropic layer model

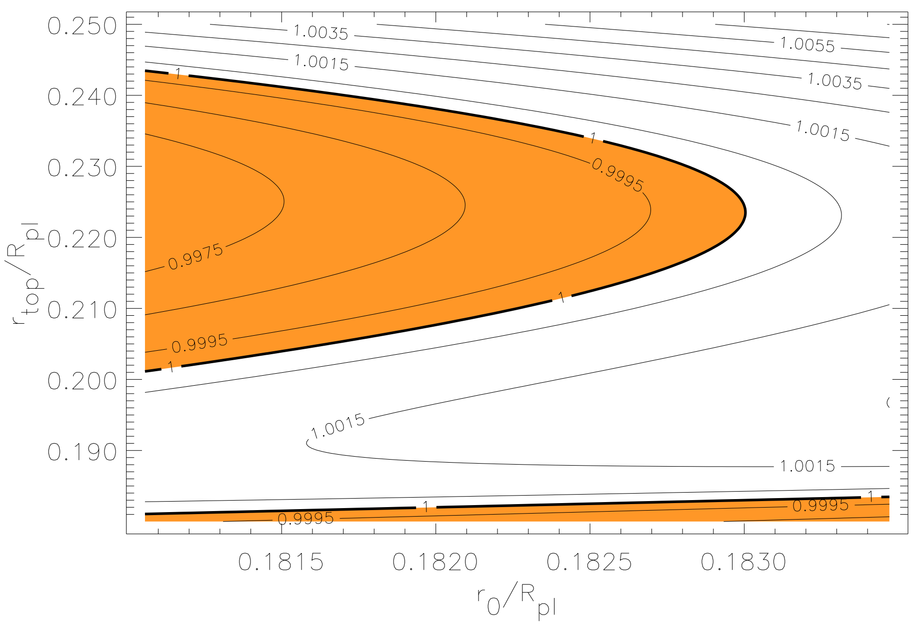

simulation

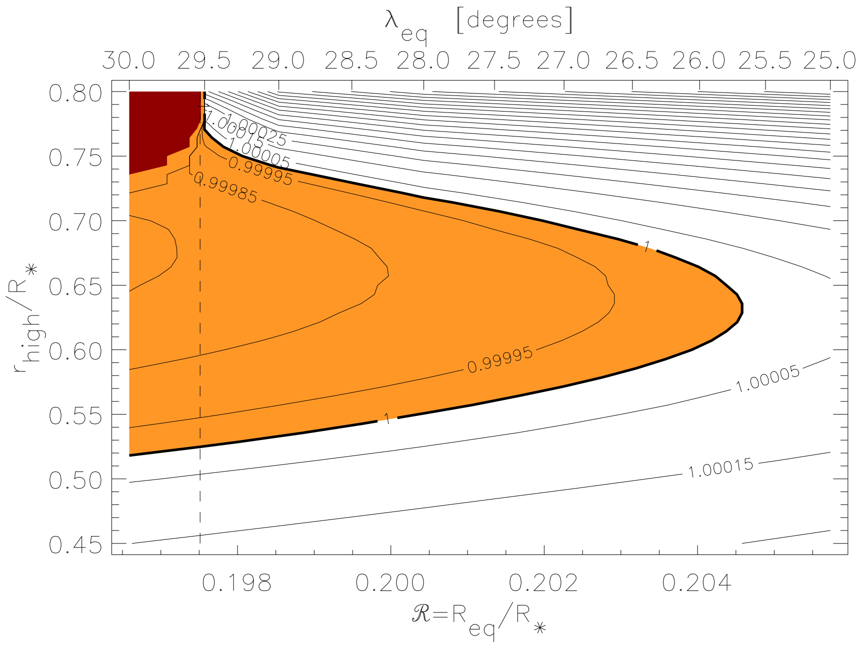

$R_{\rm pl}$: radius of polytropic sphere

Radial trajectories

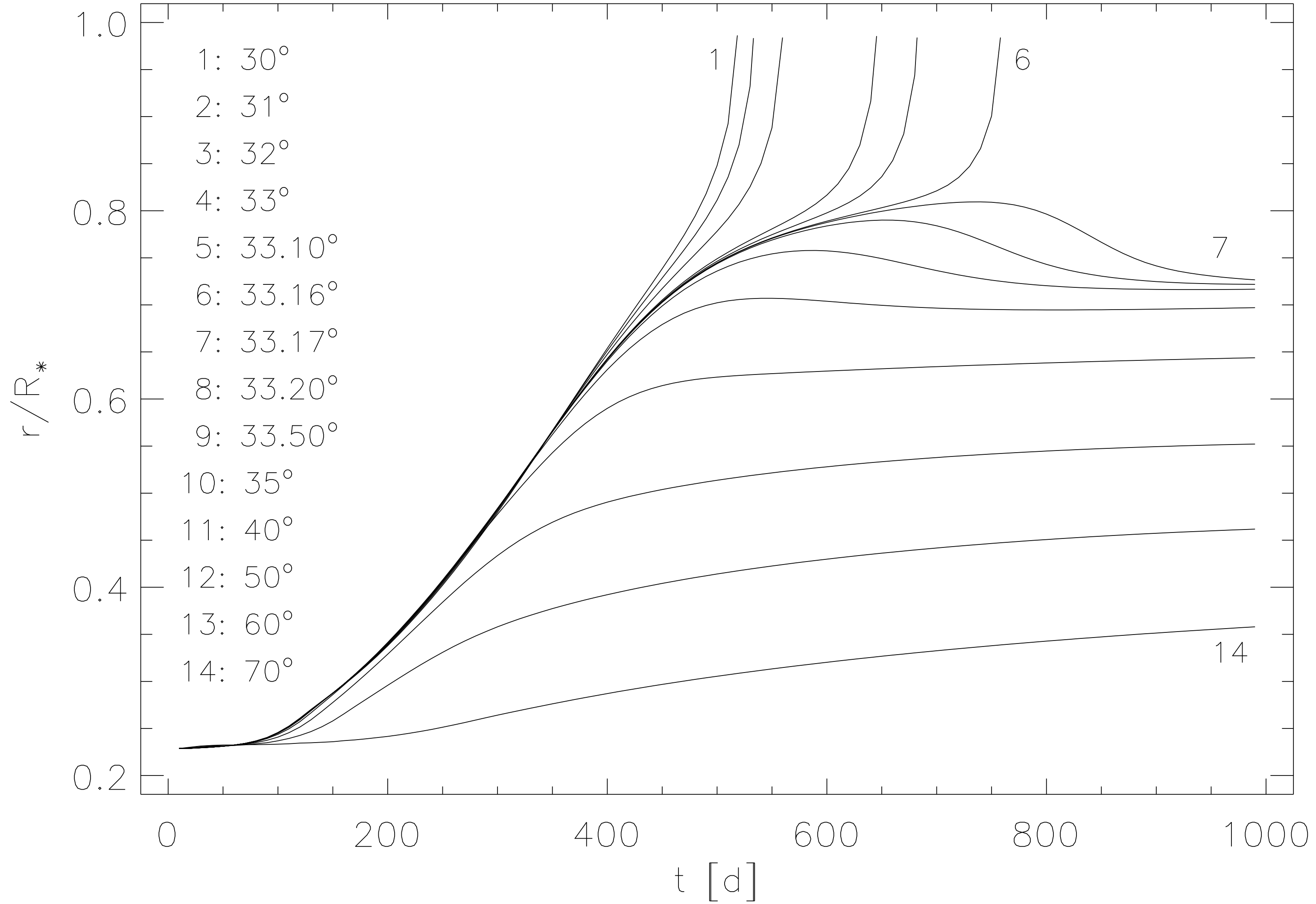

$M_* = 1 M_\odot$ (#540, 12.14 Gyr), $B = 2 \cdot 10^5$ G, $\lambda_{\rm crit} \simeq 33.16^{\rm o}$

Parameter dependence

Hardly any dependence of the trapping mechanism on

- rotation rate
- growth time / initial magnetic field strength
- magnetic flux / drag force
- initial depth of equilibrium
- detailed stellar stratification

$\Rightarrow$ Trapping mechanism dominated by $\mathcal{R} = R_{\mathrm{eq}}/R_{*} \propto r_{\mathrm{core}}/R_{*}$
i.e. depends on **evolutionary stage** of the post-MS star

Importance for the ‘Coronal Dividing Line’

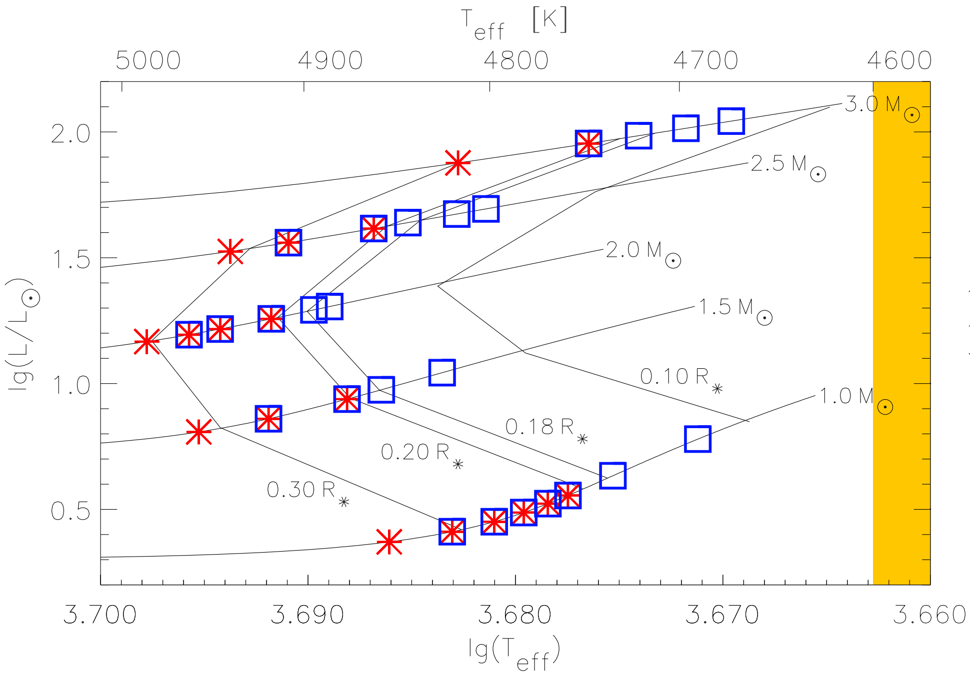

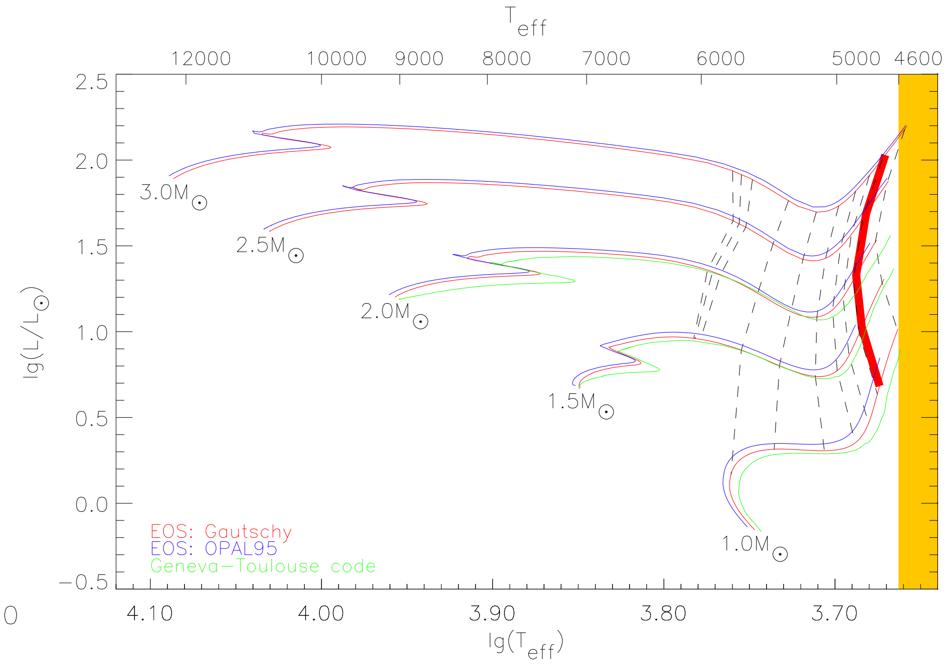

- trapping of flux tubes at all latitudes for $r_{\text{core}} < 0.18 \ldots 0.2\,\mathrm{R}_*$ ($T_{\text{eff}} = 4750 \ldots 4900\,\mathrm{K} \Rightarrow$ G7–K0, close to the left of the CDL)

$\Rightarrow$ **Flux tube trapping** is an explanation for ‘Coronal Dividing Line’

Summary

- Observations: decrease of coronal X-ray emission for giants cooler than spectral type K0-K3 $\Longrightarrow$ Coronal Dividing Line (CDL)
- Theory: change of coronal magnetic field structure from closed, large-scale coronal loops to mainly open field lines
- Simulations: onset of flux tube trapping in HRD $\approx$ CDL
- Result: change from closed to open field structure can be explained by the *'buried flux tube'* model.

Drag instability

- *Simulations:* **unexpected** eruptions of assumed stable magnetic flux tubes
- *Reason:* aerodynamic drag force $\mathbf{f}_{\rm drag}$
  - $|\mathbf{f}_{\rm drag}| \propto v_\perp^2$
  - higher-order effect, vanishes in stability analysis after linearization
- *'Horizontal flux tube' model:*
  - $|\mathbf{f}_{\rm drag}| \propto v_\perp$ (**Stokes** ansatz)
  - external tangential flow velocity v
  - wave mode with phase velocity $v_{\rm phs}$
  - **drag instability** for $v > v_{\rm phs}$

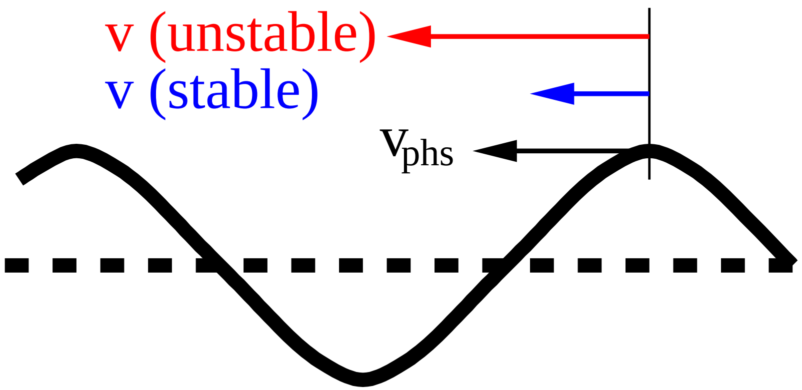

$\Rightarrow$ 'negative-energy waves', Ryutova M.P., 1988, Sov. Phys. JETP **67** (8)

Instability mechanism

- Stokes drag force:

  $\mathbf{f}_{\mathrm{drag}} \propto -\mathbf{v}_{\mathrm{rel}}$

- blue: damped wave mode

  red: growing wave mode

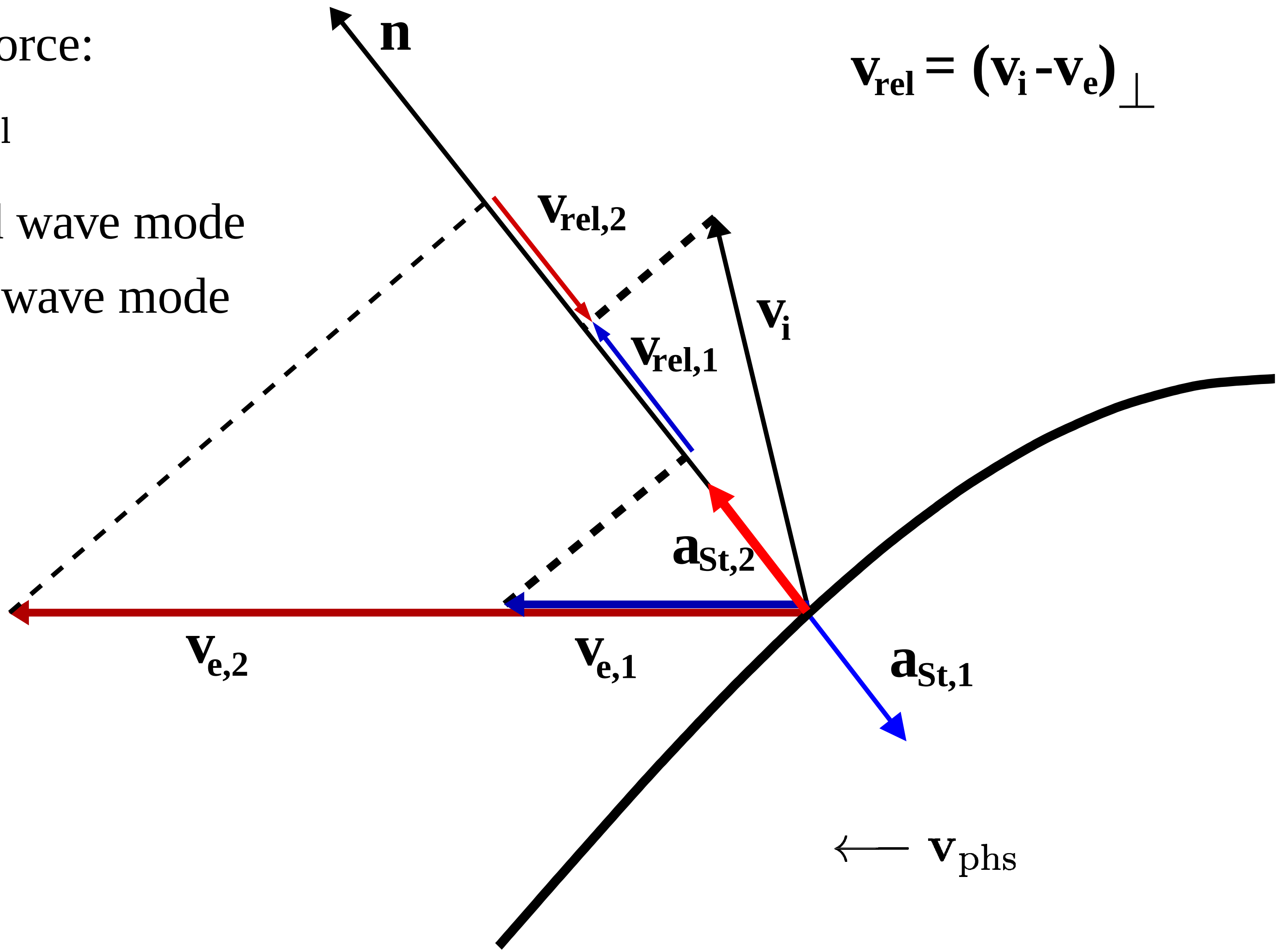

Growth times ($M_* = 1\,\mathrm{M}_\odot, T = 2\,\mathrm{d}$)

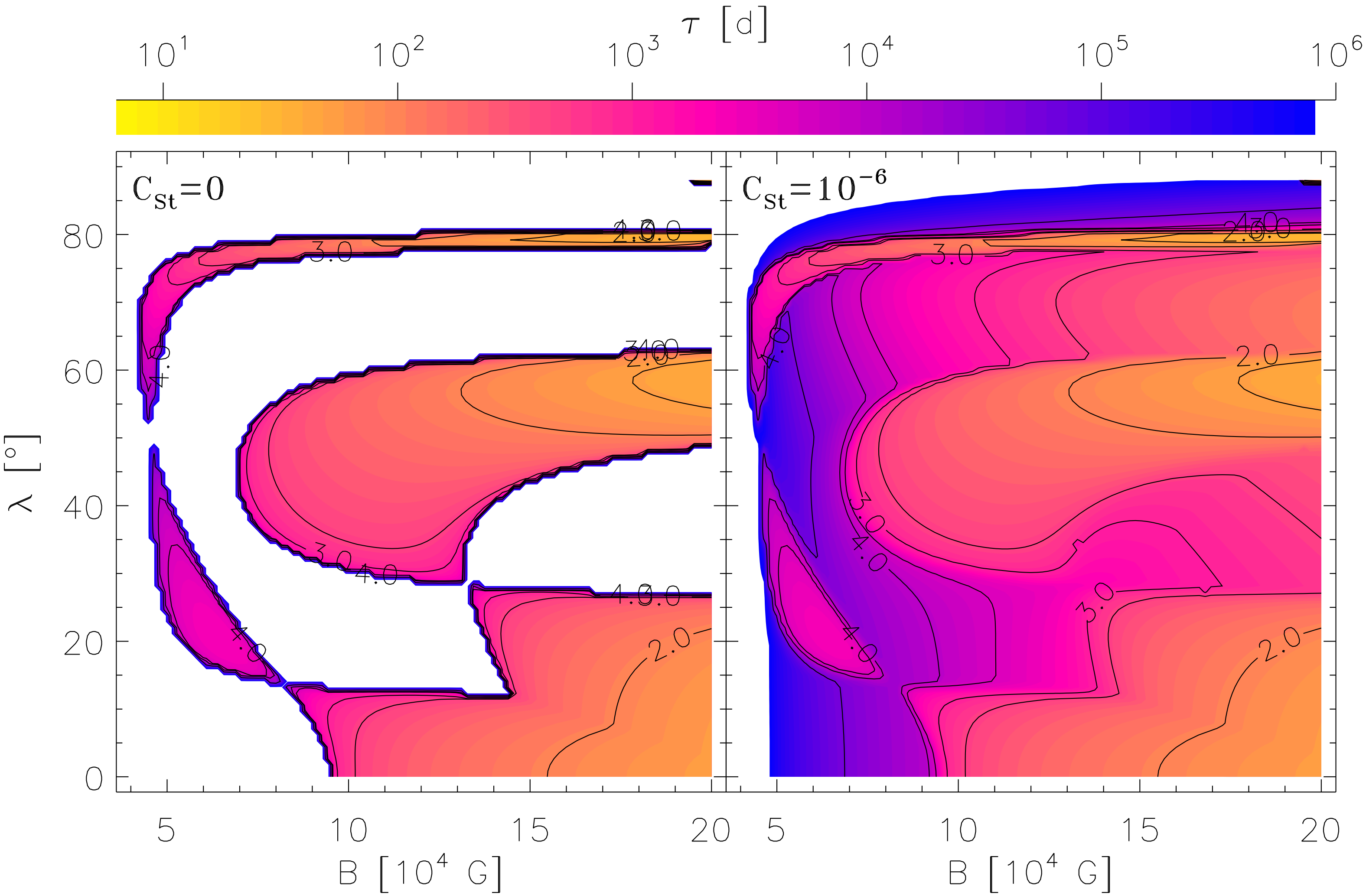

$\log_{10}\tau$-levels for $\tau = 10, 50, 100, 500, 10^3, 5\cdot10^3, 10^4, 5\cdot10^4$

Growth times ($M_* = 1\,\mathrm{M}_\odot, T = 27\,\mathrm{d}$)

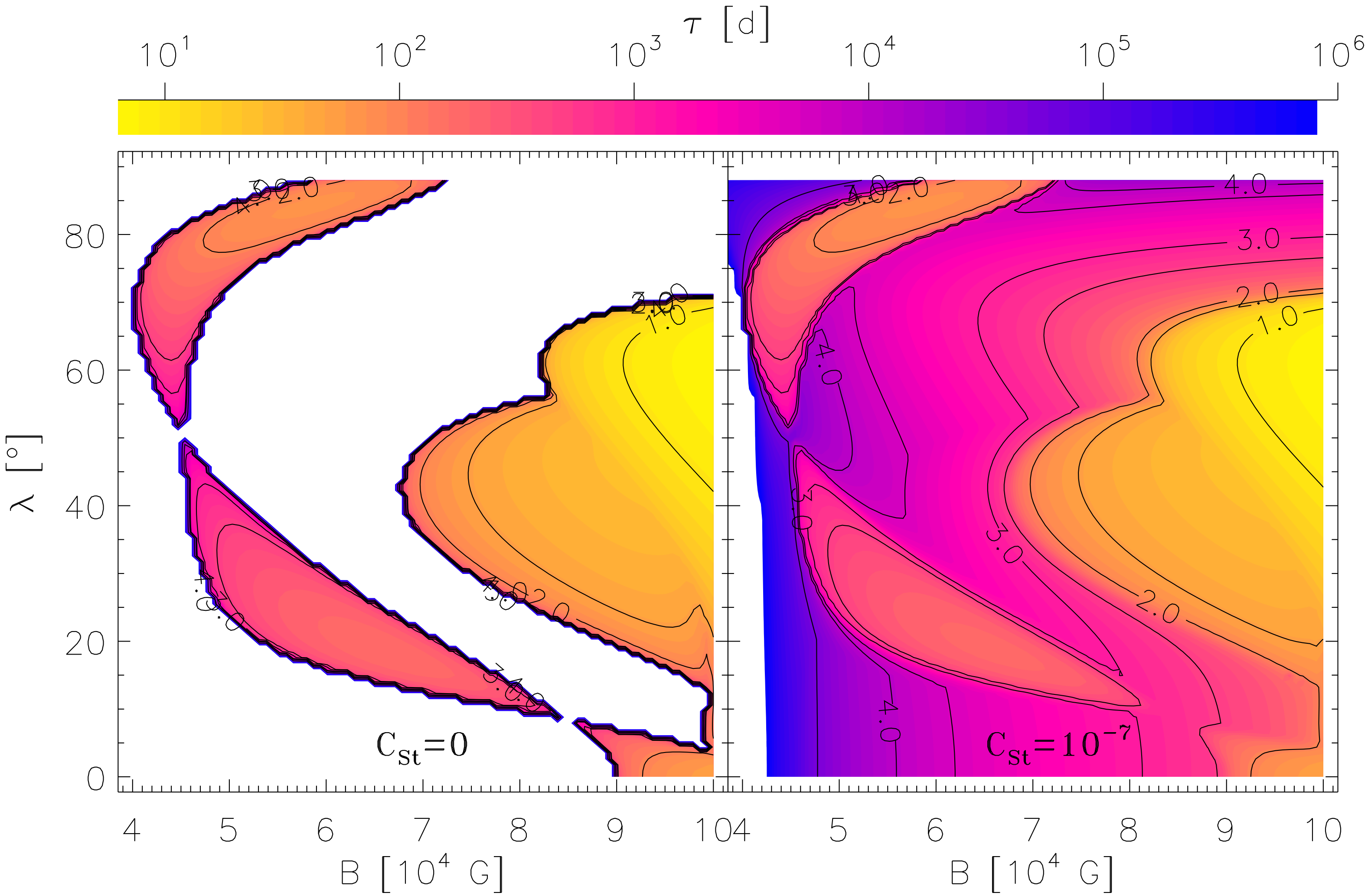

$\log_{10}\tau$-levels for $\tau = 10, 50, 100, 500, 10^3, 5\cdot10^3, 10^4, 5\cdot10^4$

Summary

- *Flux tubes in giant stars:*

  Trapping of flux tubes in cool giants stars explains the fading of coronal X-ray emission across the ‘Coronal Dividing Line’

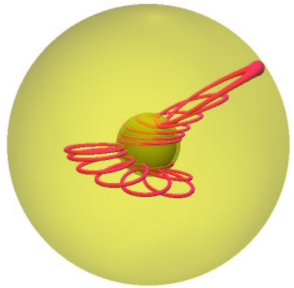

- *Flux tubes in binary stars:*

  Considerable non-uniformities and preferred longitudes in spot distributions due to tidal effects

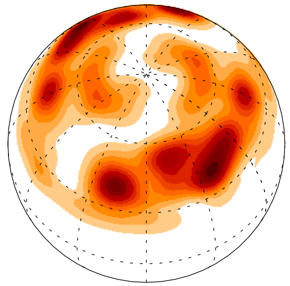

- *Drag instability:*

  General instability mechanism presumably relevant for the storage of magnetic flux tubes